



USAF TPS L-23 Shear Wind Observed Optimized Path Investigation for NASA (SENIOR ShWOOPIN)

**A
F
F
T
C**

Randy Gordon, Capt, USAF
Project Manager/Project Pilot

Robert Fails, Maj, USMC
Project Pilot

Solomon Baase, Capt, USAF
Project Pilot

Jason Eckberg, Capt, USAF
Flight Test Navigator

Charles Ryan, Capt, USAF
Flight Test Engineer

Chris Smith, Capt, USAF
Flight Test Engineer

June 2006

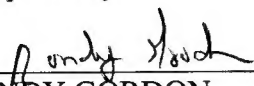
FINAL TECHNICAL INFORMATION MEMORANDUM

Approved for public release; distribution is unlimited.

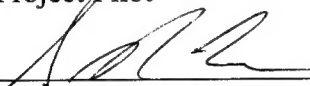
AIR FORCE FLIGHT TEST CENTER
EDWARDS AIR FORCE BASE, CALIFORNIA
AIR FORCE MATERIAL COMMAND
UNITED STATES AIR FORCE


This Technical Information Memorandum (AFFTC-TIM-06-02, SENIOR ShWOOPIN) was prepared and submitted under Job Order Number M06C0100 by the SENIOR ShWOOPIN test team.

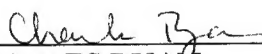
Prepared by:



RANDY GORDON
Captain, USAF
Project Manager/Project Pilot


ROBERT FAILS
Major, USMC
Project Pilot

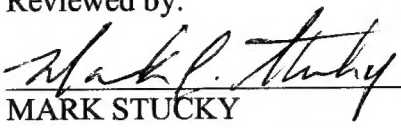

SOLOMON BAASE
Captain, USAF
Project Pilot

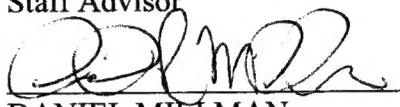

JASON ECKBERG
Captain, USAF
Flight Test Navigator

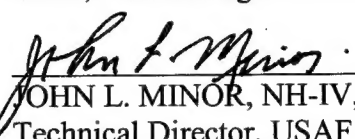

CHARLES RYAN
Captain, USAF
Flight Test Engineer


CHRIS SMITH
Captain, USAF
Flight Test Engineer

Reviewed by:


MARK STUCKY
Lieutenant Colonel, USAF
Staff Advisor


DANIEL MILLMAN
Lieutenant Colonel, USAF, PhD
Chief, Test Management Branch


JOHN L. MINOR, NH-IV, DAF
Technical Director, USAF Test Pilot School

Approved by:

JUN 8 2007


ANDRE A. GERNER, Colonel, USAF
Commandant, USAF Test Pilot School

REPORT DOCUMENTATION PAGEForm Approved
OMB No. 0704-0188

Public reporting burden for this collection of information is estimated to average 1 hour per response, including the time for reviewing instructions, searching existing data sources, gathering and maintaining the data needed, and completing and reviewing this collection of information. Send comments regarding this burden estimate or any other aspect of this collection of information, including suggestions for reducing this burden to Department of Defense, Washington Headquarters Services, Directorate for Information Operations and Reports (0704-0188), 1215 Jefferson Davis Highway, Suite 1204, Arlington, VA 22202-4302. Respondents should be aware that notwithstanding any other provision of law, no person shall be subject to any penalty for failing to comply with a collection of information if it does not display a currently valid OMB control number. PLEASE DO NOT RETURN YOUR FORM TO THE ABOVE ADDRESS.

| | | | | | |
|---|------------------------------------|---|---|--|---|
| 1. REPORT DATE June 2006 | | 2. REPORT TYPE Final Technical Information Memorandum | | 3. DATES COVERED (From - To) 15 March -3 May 2006 | |
| 4. TITLE AND SUBTITLE USAF TPS L-23 Shear Wind Observed Optimized Path Investigation for NASA (SENIOR ShWOOPIN) | | | | 5a. CONTRACT NUMBER | |
| 6. AUTHOR(S) Gordon, Randy, Captain, USAF Fails, Robert, Major, USMC Baase, Solomon, Capt, USAF Eckberg, Jason, Capt, USAF Ryan, Charles, Capt, USAF Smith, Chris, Capt, USAF | | | | 5b. GRANT NUMBER | |
| | | | | 5c. PROGRAM ELEMENT NUMBER | |
| | | | | 5d. PROJECT NUMBER | |
| | | | | 5e. TASK NUMBER | |
| | | | | 5f. WORK UNIT NUMBER | |
| 7. PERFORMING ORGANIZATION NAME(S) AND ADDRESS(ES) Air Force Flight Test Center 412th Test Wing USAF Test Pilot School 220 South Wolfe Ave Edwards AFB CA 93524-6485 | | | | 8. PERFORMING ORGANIZATION REPORT NUMBER AFFTC-TIM-06-02 | |
| 9. SPONSORING / MONITORING AGENCY NAME(S) AND ADDRESS(ES) Major Paul Blue AFIT/ENY Graduate School of Engineering 2950 Hobson Way, WPAFB, OH 45433-7765 | | | | 10. SPONSOR/MONITOR'S ACRONYM(S) | |
| | | | | 11. SPONSOR/MONITOR'S REPORT NUMBER(S) | |
| 12. DISTRIBUTION / AVAILABILITY STATEMENT Approved for public release; distribution is unlimited. | | | | | |
| 13. SUPPLEMENTARY NOTES CA: Air Force Flight Test Center Edwards AFB CA CC: 012100 | | | | | |
| 14. ABSTRACT The SENIOR ShWOOPIN TMP was conducted at the request of the USAF TPS as part of a NASA investigation into the viability of aircraft endurance enhancement through the extraction of energy from horizontal wind gradients. Eighty-eight test sorties were performed from 15 March -3 May 2006 under Job Order Number (JON) M06C0100. The six member SENIOR ShWOOPIN test team from TPS Class 05B performed the testing at the North Base facilities of Edwards AFB. Flight testing gathered sailplane flight state and energy height data during the course of several Dynamic Soaring maneuvers through horizontal wind shears as well as calm winds. Data were recorded and reduced post flight. | | | | | |
| 15. SUBJECT TERMS SENIOR ShWOOPIN, Dynamic Soaring, L-23 Super Blanik, Flight Testing, Atmospheric Wind Gradients, Atmospheric Energy Extraction, Wind Shear, Sailplanes, Gliders, Gliding, Wind Velocity, Aerodynamic Drag, Drag Reduction, Lift to Drag Ratio | | | | | |
| 16. SECURITY CLASSIFICATION OF: Unclassified | | | 17. LIMITATION OF ABSTRACT SAME AS REPORT | 18. NUMBER OF PAGES 76 | 19a. NAME OF RESPONSIBLE PERSON Mark Stucky, Lt Col, USAF |
| a. REPORT Unclassified | b. ABSTRACT Unclassified | c. THIS PAGE Unclassified | | | 19b. TELEPHONE NUMBER (include area code) 661-277-2125 |

Standard Form 298 (Rev. 8-98)
Prescribed by ANSI Std. Z39.18

This page intentionally left blank.

PREFACE

The SENIOR ShWOOPIN Test Management Project (TMP) was conducted by the USAF Test Pilot School as part of a joint United States Air Force and National Aeronautics and Space Administration study into the theory of extending aircraft endurance using Dynamic Soaring maneuvers in horizontal wind shears. SENIOR ShWOOPIN used a heavily modified L-23 Super Blanik to investigate this phenomenon.

The SENIOR ShWOOPIN test team would like to extend sincere thanks to Mr. James Murray and Mr. Russ Franz, NASA DFRC, for their invaluable assistance with aircraft instrumentation, data collection, and analysis. Additionally, the team would like to thank Capt. E. T. Waddell for his assistance with design of experiments. Without their help, this project could not have happened.

This page intentionally left blank.

EXECUTIVE SUMMARY

This test report presents the results of the SENIOR ShWOOPIN project. The goal of this Dynamic Soaring investigation was to prove or disprove the viability of increasing a full size sailplane's total energy by extracting energy from horizontal wind gradients. Dynamic Soaring has been used by seabirds like the albatross to fly hundreds of kilometers by extracting energy from horizontal wind shears across the ocean. Radio controlled gliders have also used this technique to achieve sustained speeds of over 200 miles per hour. Dynamic Soaring, however, has never before been studied for use on full size sailplanes. The specific objectives of this test were to compare the energy gained or lost during the "hairpin" and "anti-hairpin" maneuvers both in a wind shear and with no wind shear (baseline energy loss case), determine if full size sailplanes could extract energy from horizontal wind shears, evaluate the L-23 Super Blanik sailplane MATLAB® model for Dynamic Soaring developed at the Air Force Institute of Technology (AFIT), and to qualitatively evaluate the utility of Dynamic Soaring as a practical maneuver for large sailplanes.

The SENIOR ShWOOPIN Test Management Project (TMP) was conducted in cooperation with the National Aeronautics and Space Administration Dryden Flight Research Center (NASA DFRC) and the United States Air Force Test Pilot School (USAF TPS) as an investigation into the viability of manned sailplane and UAV endurance enhancement through the extraction of energy from atmospheric wind gradients. One hundred thirty-eight sorties in the L-23 (88 test sorties and 50 training/avionics validation flights) were performed between 15 March and 3 May 2006 under Job Order Number (JON) M06C0100. The SENIOR ShWOOPIN test team consisted of three test pilots, one flight test navigator, and two flight test engineers. Additional personnel supported the flight tests by serving as tow pilots and glider instructor pilots. Testing occurred at the North Base facilities of Edwards Air Force Base.

Two Dynamic Soaring maneuvers were derived from MATLAB® optimal path analysis and the observed flight trajectory of the albatross seabird in wind shear flight. The first maneuver was known as the hairpin and was designed to extract the most amount of energy from wind shears. The second maneuver was known as the anti-hairpin and was designed to prove the theory of Dynamic Soaring by illustrating the increase in energy loss when Dynamic Soaring was flown exactly opposite of the hairpin maneuver. Data obtained from these flight test maneuvers included specific energy height and sailplane flight states (accelerations, attitudes, velocities, etc).

The flight test data indicated that the L-23 did extract energy from the wind shear. Additionally, the results agreed with Dynamic Soaring theory, in that, a Dynamic Soaring maneuver executed into a headwind loses the least amount of energy, while a maneuver executed with a tailwind loses the most energy. However, the amount of energy extraction was small and did not provide sufficient energy to sustain flight. Conduct Dynamic Soaring tests in the stronger wind shears generated by orthographic features.

TABLE OF CONTENTS

| | |
|--|------|
| PREFACE | iii |
| EXECUTIVE SUMMARY | v |
| TABLE OF CONTENTS..... | vi |
| LIST OF FIGURES | viii |
| LIST OF TABLES | ix |
| LIST OF TABLES | ix |
| Introduction..... | 1 |
| Background | 1 |
| Program Chronology..... | 1 |
| Test Item Description..... | 1 |
| Test Objectives..... | 3 |
| Limitations | 3 |
| Test and Evaluation..... | 5 |
| General | 5 |
| Test Procedures..... | 6 |
| Dynamic Soaring Flight Test Technique (DS FTT) | 6 |
| Test Execution | 7 |
| Results and Analysis | 9 |
| Energy state comparison | 9 |
| Does Dynamic Soaring exist? | 11 |
| How does the AFIT model compare? | 12 |
| Can it be employed by glider pilots? | 16 |
| Conclusions and Recommendations | 19 |
| References..... | 21 |
| Appendix A: Instrumentation and Displays..... | A-1 |
| Sensors | A-1 |
| Guidestar GS-111m | A-1 |
| Air Data Probe | A-1 |
| Resistive Temperature Detector..... | A-2 |
| Surface Position Transducers..... | A-2 |
| GS-111m Interface..... | A-2 |
| Laptop PC Interface | A-2 |
| Tablet PC | A-3 |
| Point-to-Point Protocol Terminal..... | A-3 |
| Data Acquisition | A-3 |
| Tablet PC Display | A-4 |
| Appendix B: MATLAB® Data Reduction Methodology | B-1 |
| Appendix C: Design of Experiments Analysis | C-1 |
| Appendix D: Lessons Learned..... | D-1 |
| Facilities/Lakebed Operations | D-1 |
| Airfield Management Coordination..... | D-1 |
| Weather Support | D-1 |
| Instrumentation/Displays | D-2 |
| Simulator..... | D-2 |

| | |
|---|-----|
| Appendix E: Total Energy Probe Theory | E-1 |
| Appendix F: Flight Test Results | F-1 |
| Appendix G: Data Anomalies | G-1 |
| Appendix H: Energy Height Plot Description | H-1 |
| Appendix I: Plots of Energy Height Lost Using the Averaging Method..... | I-1 |
| Appendix J: Cooper-Harper Rating Scale..... | J-1 |
| Appendix K: Acronym List | K-1 |

LIST OF FIGURES

| | |
|--|-----|
| Figure 1: L-23 Super Blanik Test Aircraft with Mobile Operations Center..... | 2 |
| Figure 2: Front (left) and Rear (right) Cockpit Displays Panels..... | 2 |
| Figure 3: NASA DFRC Glider Simulator..... | 5 |
| Figure 4: Dynamic Soaring Maneuver..... | 6 |
| Figure 5: Glider Operating Area at North Base..... | 8 |
| Figure 6: 85 Knot Entry Speed Glider Simulator and Flight Test Comparison (Pilot 1) | 13 |
| Figure 7: 95 Knot Entry Speed Glider Simulator and Flight Test Comparison (Pilot 1) | 14 |
| Figure 8: 105 Knot Entry Speed Glider Simulator and Flight Test Comparison (Pilot 1) | 15 |
| Figure 9: Cooper-Harper Ratings..... | 17 |
| Figure A-1: Tablet PC Display | A-4 |
| Figure B-1: Sample Plot of Pitot-static and Geometric Energy Height..... | B-2 |
| Figure B-2: Sample Plot of Indicated Airspeed, Ground Speed and Altitude | B-3 |
| Figure B-3: Sample Plot of Body Fixed Velocities | B-4 |
| Figure B-4: Sample Plot of Inertial Velocities | B-5 |
| Figure B-5: Sample Plot of Euler Angle Rates..... | B-6 |
| Figure B-6: Sample Plot of Euler Angles | B-7 |
| Figure B-7: Sample Plot of Inertial Position Relative to Maneuver Point | B-8 |
| Figure B-8: Sample Plot of Sailplane Ground Track and Altitude..... | B-9 |
| Figure C-1: Plot of the Chances of Missing a Difference in Energy Height | C-2 |
| Figure H-1: Hairpin Maneuver Pitot-static and Geometric Energy Loss in a Horizontal Wind Shear | H-1 |
| Figure H-2: Anti-Hairpin Maneuver Pitot-static and Geometric Energy Loss in a Horizontal Wind Shear..... | H-2 |
| Figure H-3: No Shear Dynamic Soaring Maneuver Pitot-static and Geometric Energy Loss .. | H-3 |
| Figure I-1: Pitot-static Energy Height Losses for 85 KIAS Maneuvers..... | I-1 |
| Figure I-2: Geometric Energy Height Losses for 85 KIAS Maneuvers | I-2 |
| Figure I-3: Pitot-static Energy Height Losses for 95 KIAS Maneuvers..... | I-3 |
| Figure I-4: Geometric Energy Height Losses for 95 KIAS Maneuvers | I-4 |
| Figure I-5: Pitot-static Energy Height Losses for 105 KIAS Maneuvers..... | I-5 |
| Figure I-6: Geometric Energy Height Losses for 105 KIAS Maneuvers | I-6 |

LIST OF TABLES

| | |
|---|-----|
| Table 1: Average Final Energy Height Loss of the Hairpin Maneuver in Wind Shear (ft)..... | 10 |
| Table 2: Average Final Energy Height Loss in No Shear (ft) | 10 |
| Table 3: Average Final Energy Height Loss of the Anti-Hairpin Maneuver in Wind Shear (ft) . | 10 |
| Table C-1: DOE Factors Considered | C-1 |
| Table C-2: Pitot-static Energy Model Statistics..... | C-1 |
| Table F-1: 80-90 KIAS Entry Speed Data Points..... | F-2 |
| Table F-2: 90-100 KIAS Entry Speed Data Points..... | F-3 |
| Table F-3: 100-110 KIAS Entry Speed Data Points..... | F-4 |

This page intentionally left blank.

Introduction

Background

Dynamic Soaring is a soaring technique that extracts energy from shear in horizontal winds. Seabirds, like the albatross, have demonstrated the viability of Dynamic Soaring by staying aloft for hundreds of kilometers by adding energy to their flight without flapping their wings. Radio controlled gliders have also used Dynamic Soaring techniques to achieve sustained speeds of over 200 miles per hour. However, energy states during Dynamic Soaring maneuvers have never before been quantified with respect to full size gliders. This test quantified the energy state of the glider throughout the execution of Dynamic Soaring maneuvers. Comparisons were made between the Dynamic Soaring maneuver, called the “hairpin”, and the anti-Dynamic Soaring maneuver, called the “anti-hairpin”, to determine the magnitude of energy state changes.

Previous United States Air Force Test Pilot School (TPS) test management projects (TMP) documented the performance and stability derivatives of the L-23 sailplane in preparation for this project. In 2004, the SENIOR IDS project team collected flight test data to determine the lift and drag polars of the L-23. The HAVE BLADDER project team determined the sailplane’s stability derivatives and moments of inertia in 2005.

The Shear Wind Observed Optimized Path Investigation for NASA (SENIOR ShWOOPIN), a team of USAF TPS students, conducted testing using the same L-23 sailplane. The test team examined the feasibility of extracting energy from horizontal wind shears in cooperation with NASA Dryden Flight Research Center (DFRC). Test results were also used for evaluation of an Air Force Institute of Technology (AFIT) thesis model. All testing was accomplished under the M06C0100 JON (job order number).

Program Chronology

One hundred thirty-eight sorties in the L-23 (88 test sorties and 50 training/avionics validation flights) were performed between 15 March and 3 May 2006. A total of 27 hours of flight test were accomplished.

Test Item Description

The L-23 was designed and manufactured by LET Aeronautics Works in the Czech Republic and was marketed in the United States by Blanik America, Wenatchee, WA. The two-place, tandem cockpit L-23 was owned by the USAF TPS and made of an all metal structure. The rudder, elevator, and ailerons were fabric covered. The T-tail was fitted with a conventional elevator and pitch trim tab for pitch control. The main landing gear on the test aircraft was pinned down and the cockpit gear handle had been removed. The L-23 glide ratio was 24:1 at approximately 48 KIAS with the speedbrake retracted and the landing gear extended. The conventional three axis flight control system was non-powered and fully reversible. Both cockpits were equipped with a center mounted control stick and rudder pedals that actuated control surfaces with a combination of control push rods and cables. The speedbrakes were controlled by levers from either cockpit. The never exceed airspeed was 133 KIAS. Load factor limits were -2.5 to +5.3 g at full gross weight (1124 pounds with two occupants).



Figure 1: L-23 Super Blanik Test Aircraft with Mobile Operations Center

The aircraft was modified with a data acquisition system (DAS) consisting of a five-hole Pitot-static probe, an inertial measurement unit (IMU), two tablet PCs displaying real time attitude, load factor, flight altitude, and specific energy height (E_s) information, a digital readout of energy height from the total energy variometer probe (rear cockpit), and a digital cockpit camera. For background theory regarding the total energy variometer reference Appendix E: Total Energy Probe Theory.



Figure 2: Front (left) and Rear (right) Cockpit Displays Panels

The total weight of modification equipment was 22 pounds allowing for a maximum combined weight of 396 pounds for crewmembers. The DAS was completely independent of the production Pitot-static system. The boom mounted five-hole Pitot-static probe had a hemispherical tip, and measured total and differential pressure, provided airspeed, altitude, angle of attack (AOA), and angle of sideslip (AOS) signals. The digital camera was mounted behind the pilot station to record over the shoulder video. The software on the tablet PC also provided the capability to playback recorded data post flight. The IMU was installed in the baggage compartment behind the rear cockpit. The unit was a battery-powered GS-111m produced by

Athena Technologies, Inc, Warrenton, VA. It incorporated the sensor suite necessary to provide a full attitude, navigation, and air data solution for use in vehicle flight-state measurement.

The GS-111m was equipped with accelerometers, angular rate sensors, and magnetometers in all three axes, an internal GPS receiver, and air data sensors. A real-time, multi-state Kalman filter was used to integrate the different sensors. The aircraft also had a VHF radio to communicate with other aircraft and ground stations. Refer to Appendix A: Instrumentation and Displays for more detailed information. The performance of the L-23 under test was considered production representative.

Test Objectives

The overall test objectives for this project were four-fold and are listed below.

1. Compare the energy gained or lost during the hairpin and anti-hairpin maneuvers, both in a wind shear and without wind shear (baseline energy loss case).
2. Determine if full size sailplanes can extract energy from horizontal wind shears.
3. Evaluate the L-23 sailplane MATLAB[®] model for Dynamic Soaring developed at the Air Force Institute of Technology (AFIT).
4. Qualitatively evaluate the utility of Dynamic Soaring as a practical maneuver for large sailplanes.

Limitations

None.

This page intentionally left blank.

Test and Evaluation

General

The unique nature of this project necessitated the development of specific flight test techniques, data collection methods, and mission-specific avionics. These techniques, methods, and avionics were all first tested on the NASA DFRC glider simulator. Using the L-23 sailplane aerodynamic drag polar data developed by a previous USAF TPS Test Management Project (reference 1) in 2004 and the L-23 sailplane stability derivatives and moments of inertia calculated by another USAF Test Management Project (reference 2) in 2005, the SENIOR ShWOOPIN test team began its investigation of Dynamic Soaring by developing an L-23 Dynamic Soaring flight simulator.



Figure 3: NASA DFRC Glider Simulator

Using this flight simulator, the test team was able to practice the Dynamic Soaring flight test techniques in various wind shears, refine crew coordination procedures, verify and validate in-house developed Dynamic Soaring flight displays and avionics, and collect data to be used for a comparison analysis between flight and simulation. Following simulator ground testing, the tablet PC displays were installed into the sailplane on 13 March 2006 and the avionics validation flights were completed by 26 March 2006.

The test team crew solo checkout consisted of a total of seven flights per individual and covered standard sailplane operations, sailplane flying and handling qualities familiarization, emergency procedures, Dynamic Soaring practice, and North Base/North Rogers Dry Lake area orientation flights. In total, 50 training/avionics validation sorties were flown between 15 March 2006 and 7 April 2006.

The test window began on 10 April 2006 and continued through 3 May 2006. A total of 135 test points were flown at the North Base facilities of Edwards AFB for a total of 27 hours of flight test.

Test Procedures

Dynamic Soaring Flight Test Technique (DS FTT)

The Dynamic Soaring flight test technique (DS FTT) developed for this project was selected to optimize energy extraction from horizontal wind shear while at the same time ensuring repeatability, and simplifying data analysis. The energy states at the beginning and end of the maneuver could be directly compared because no axis transformations had to be accomplished. Three airspeeds were used to enter the maneuver; 85, 95, 105 KIAS. These airspeeds were chosen based off of an L-23 MATLAB[®] model developed for this research project. The DS FTT was initiated from wings level flight at the target entry airspeed, perpendicular to the wind, and at the bottom of the wind shear gradient. The pilot smoothly rolled and pulled to execute a 45 to 90 degree heading change simultaneous with a 15 to 25 degree pitch up. For an entry airspeed of 85 KIAS the pitch up was 15-20 degrees, and for a 95 or 105 KIAS entry the pitch up was 20-25 degrees. As airspeed decreased in the climb the pilot reversed the turn and rolled the aircraft to approximately 50 degrees of bank across the apex of the maneuver. At the apex of the maneuver the nose was near the horizon and the glider was back on the maneuver entry heading. Minimum airspeed over the top was 40 KIAS, and the apex altitude was 200-400 feet above the entry altitude. As the glider was turned back towards the original ground track the nose was allowed to drop to 15 to 25 degrees nose low (amount of nose low attitude matched the amount of nose high attitude on the first leg of the maneuver). As the glider descended the pilot again reversed the roll and pulled to fly back to the initial heading and altitude. The maneuver ended with the glider on the entry heading and altitude with the wings level. Figure 4 shows a 3-dimensional plot of the ground and altitude track of a representative DS FTT maneuver. A hairpin maneuver was defined by flying the DS FTT with a climb into a headwind and a descent with a tailwind. An anti-hairpin maneuver was defined by flying the DS FTT with a climb into a tailwind and a descent with a headwind.

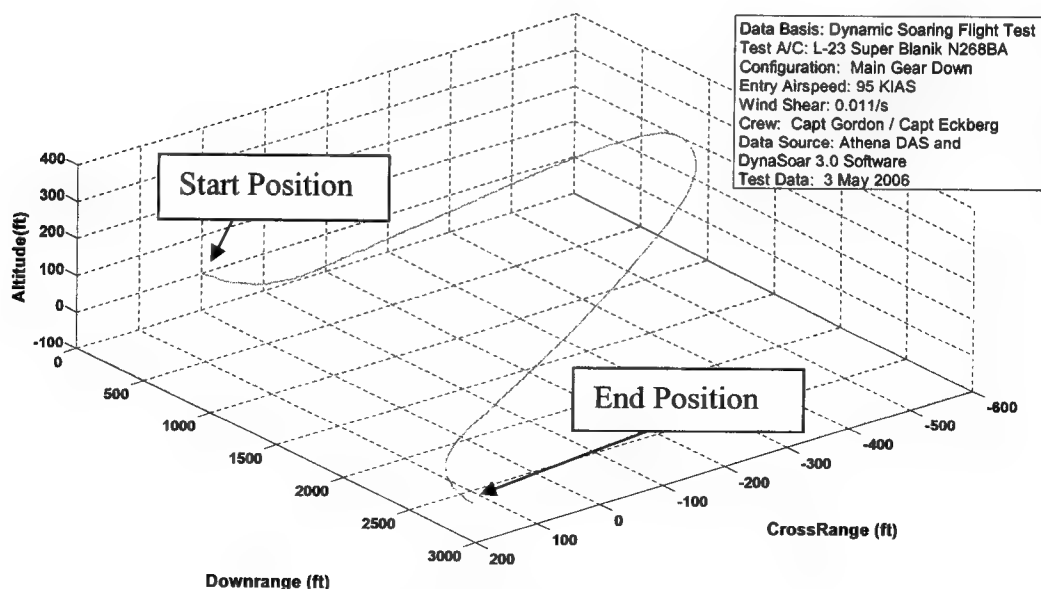


Figure 4: Dynamic Soaring Maneuver

During each maneuver, the rear cockpit crewmember provided maneuver clearance based on data band and tolerances established in the test plan, recorded total energy height directly from the total energy gauge at entry, apex, and exit of the maneuver, and provided altitude pacing calls to ensure maneuvers ended at the altitude where the maneuvers started. Additionally, the FTE/N monitored the energy state of the glider to ensure the total energy did not drop below the minimum allowed maneuver energy.

Test Execution

Each test period started with an initial crew briefing, lakebed inspection, weather balloon launch, operations setup, and instrumentation check. Forecast soundings were briefed to the crews to give a general idea as to where the strongest wind shear layer was predicted. Wind shear data were collected periodically with weather balloons. Sonic Detection and Ranging (SODAR) equipment was used to monitor thermal activity. The weather balloon sent raw data including wind direction, wind speed, geopotential altitude, and temperature to a mobile ground station. Two weather technicians downloaded this data and processed it to provide plots of pressure altitude against wind direction and speed. The air temperature was required to determine if an inversion was present—typically a good indication of a shear layer. Weather information was updated at least every 60 minutes, or more frequently based on observed changes in atmospheric conditions.

Target altitudes, highlighting the appropriate shear conditions, were briefed to the crew immediately prior to launch, or radioed to a crew already on tow. To ensure rapid communication of the appropriate initial conditions for each DS FTT maneuver, a standardized format for transmitting the initial conditions were developed and reported in the form of a “4-Line” brief. The 4-Line consisted of 1) initial run in heading, 2) altitude targeted, 3) airspeed required, and 4) the wind direction.

While the weather information was being collected, the mobile operations center (see Figure 1) was driven out to the lakebed and the glider and towplane were prepared for launch. During the glider rollout, the IMU, instrumentation suite, and the avionics suite were powered on and aligned. Normal alignment took approximately 10 minutes. Ground power from the mobile operations center was connected to the glider to extend battery life of the avionics displays. Edwards tower was notified that North Base glider operations were commencing, activating the applicable range operations area (see Figure 5).



Figure 5: Glider Operating Area at North Base

A modified glider aircrew checklist was run by each crew flying the L-23 prior to each tow. The checklist included the standard glider checklist, selection of “red” or “green” lakebed conditions on the tablet PC to provide the correct minimum energy height display, and synchronization of AGL energy height on front and rear cockpit tablet PC displays (see items 7 and 10 in Figure A-1: Tablet PC Display). When these checks were complete, the glider aircrew signaled for launch, and the glider was subsequently towed to an altitude approximately 1,000 feet above the first target altitude. This provided time for the aircrew to initiate a dive to stabilize at the target airspeed, and, at crew discretion, practice the DS FTT prior to execution.

After each required test point was accomplished, the glider was recovered to the lakebed, and the crew was either re-launched, or the crew was switched out. Qualitative comments were captured immediately upon landing to provide insight into what indications were present upon shear boundary entry and techniques to improve DS FTT execution.

Results and Analysis

This test program successfully accomplished the first known scientific investigation into Dynamic Soaring using a full size aircraft. There were four primary test objectives. 1) Compare the energy states at the initial and final conditions of hairpin and anti-hairpin maneuvers with shear and without wind shear. 2) Determine if energy could be extracted from horizontal wind shear. 3) Evaluate the L-23 sailplane MATLAB® model for Dynamic Soaring as developed at the Air Force Institute of Technology (AFIT). 4) Qualitatively evaluate the utility of Dynamic Soaring as a practical maneuver for large sailplanes. All objectives were met.

Test point selection and data analysis were accomplished through the use of design of experiments (DOE). The test points were selected to vary the controllable factors of crew (pilot + engineer), initial entry airspeed, and hairpin or anti-hairpin maneuver. One variable not controlled by the test team was the wind shear. At the end of the project 135 data points were collected. Two different methods were used to analyze the data. First, the data were blocked by pilot and averaged for each flight condition. Second, a general linear model analysis was performed using DOE. In both cases, the critical factors identified in the calculated energy height were maneuver type (hairpin versus anti-hairpin), wind shear magnitude, and entry airspeed. For more information on the DOE employed in the course of this investigation see Appendix C: Design of Experiments Analysis.

Energy state comparison

The team compared the energy gained or lost during the hairpin and anti-hairpin maneuvers both in a wind shear and with no wind shear. No wind shear provided the baseline energy loss condition. This objective required the tracking of sailplane energy height during hairpin and anti-hairpin maneuver execution. Tracking energy height was accomplished using two different data sources: Pitot-static and geometric inertial data from the IMU. The Pitot-static method used the Athena DAS system to record in-flight information provided by the five-hole Pitot-static probe and the temperature probe. These data were used in the following approximation to the energy height equation derived from energy theory:

$$ES_{\text{Pitot-static}} = H_i + \frac{V_i^2}{2g}$$

In this equation it was assumed V_i (indicated airspeed) = V_c (calibrated airspeed) and V_c was converted to V_e (equivalent airspeed), which was converted to V_t (true airspeed).

Geometric energy height was determined by using the Athena DAS to record inertial based velocities and altitude for every maneuver. The IMU parameters recorded were:

- Velocity in the inertial z-axis (North) acceleration – V_z
- Velocity in the inertial x-axis (East) acceleration – V_x
- Velocity in the inertial y-axis (down) acceleration – V_y
- Geometric altitude above the ground – h_g

The following formula was used to calculate geometric energy height:

$$Es_{\text{geometric}} = H_g + \frac{V_g^2}{2g} \text{ where } V_g (\text{ground_velocity}) = \sqrt{V_x^2 + V_y^2 + V_z^2}$$

Table 1 through Table 3 summarize the results of the averaging analysis method and illustrate the differences detected in the final energy state of the sailplane for each test point. These data were compiled from MATLAB® plots generated for each flight. Reference Appendix B: MATLAB® Data Reduction Methodology for example plots.

According to Dynamic Soaring theory executing a hairpin maneuver in a wind shear should result in a final energy state higher than executing the hairpin or anti-hairpin maneuver in no wind shear. Likewise, executing these maneuvers in no wind shear should result in a higher final energy than executing the anti-hairpin maneuver in a wind shear. The average final energy (from Pitot-static and geometric sources) for each set of maneuvers was calculated for each pilot and is shown in Table 2. Maneuvers were considered to have been conducted in a shear when the change in wind speed was greater than 1.5 feet/second/100 feet (0.015 /second) [~0.9 knot/100 feet]. Any wind shear measured below 1 feet/second/100 feet (0.01 /second) [~0.5 knot/100 feet] was considered a no shear condition. The maximum wind shear noted throughout the test program was a shear of 0.04 /second [~2.5 knots/100 feet]. The data points collected during the test window are detailed in Appendix F: Flight Test Results. Data points that were discarded from the averaging analysis method are described in Appendix G: Data Anomalies.

Table 1: Average Final Energy Height Loss of the Hairpin Maneuver in Wind Shear (ft)

| AIRSPEED | 85 KIAS | | 95 KIAS | | 105 KIAS | |
|-----------|---------------------|------------------|---------------------|------------------|---------------------|------------------|
| Es SOURCE | Pitot-static ΔEs | Geometric ΔEs | Pitot-static ΔEs | Geometric ΔEs | Pitot-static ΔEs | Geometric ΔEs |
| Pilot 1 | 110 | 105 | 180 | 169 | 163 | 169 |
| Pilot 2 | 130 | 132 | 172 | 175 | 206 | 208 |
| Pilot 3 | 132 | 131 | 132 | 139 | 177 | 175 |

Table 2: Average Final Energy Height Loss in No Shear (ft)

| AIRSPEED | 85 KIAS | | 95 KIAS | | 105 KIAS | |
|-----------|---------------------|------------------|---------------------|------------------|---------------------|------------------|
| Es SOURCE | Pitot-static ΔEs | Geometric ΔEs | Pitot-static ΔEs | Geometric ΔEs | Pitot-static ΔEs | Geometric ΔEs |
| Pilot 1 | 119 | 121 | 150 | 161 | 197 | 211 |
| Pilot 2 | 151 | 154 | 160 | 172 | 225 | 248 |
| Pilot 3 | 124 | 126 | 139 | 140 | 189 | 181 |

Table 3: Average Final Energy Height Loss of the Anti-Hairpin Maneuver in Wind Shear (ft)

| AIRSPEED | 85 KIAS | | 95 KIAS | | 105 KIAS | |
|-----------|---------------------|------------------|---------------------|------------------|---------------------|------------------|
| Es SOURCE | Pitot-static ΔEs | Geometric ΔEs | Pitot-static ΔEs | Geometric ΔEs | Pitot-static ΔEs | Geometric ΔEs |
| Pilot 1 | 122 | 114 | 184 | 175 | 205 | 209 |
| Pilot 2 | 147 | 147 | N/A | N/A | N/A | N/A |
| Pilot 3 | 123 | 140 | 164 | 200 | 205 | 205 |

In general, the flight test results matched expectations. Under most conditions the energy loss when executing a hairpin maneuver was less than executing the DS FTT maneuver in a no shear condition, on the order of 5-15 percent). When executing an anti-hairpin maneuver in a wind shear energy losses were generally 10-20 percent more than the energy losses flying the hairpin maneuver in a wind shear. The Pitot-static and geometric derived energy height losses trended in the same direction. The data derived from the Pitot-static system showed some anomalies for the maneuvers with 85 and 95 KIAS entry airspeeds, and the geometric energy losses showed an anomaly at the 95 KIAS entry airspeed. The Pitot-static energy lost during all three maneuvers, hairpin, anti-hairpin, and in no shear conditions, flown by pilot 3 at 85 KIAS was approximately equal. Additionally, the Pitot-static energy lost during the anti-hairpin maneuver flown by pilot 1 at 95 KIAS was 20 percent less than the energy lost during the hairpin maneuver. The Pitot-static energy lost during the no shear maneuvers flown by pilot 1 was about 30 percent less than the energy lost when flying either maneuver in a shear. The geometric energy lost for the maneuvers flown by pilot 3 at 95 KIAS also showed an increase in energy loss when flying the hairpin maneuver in a shear compared to flying the DS FTT in no shear.

The 95 KIAS data points flown by pilot 1 only included one anti-hairpin maneuver and two hairpin maneuvers. The minimal amount of data points available does not provide enough data for the averaging analysis method to make a comparison between the three different maneuvers.

It is not clear at this time why the 85 KIAS maneuvers flown by pilot 3 did not match with Dynamic Soaring theory with regard to the Pitot-static energy calculation. The maneuvers were executed within parameters and the weather data were collected near the time the maneuvers were accomplished, and therefore the data points were not discarded. When the results of all the pilots were averaged the hairpin maneuver lost less Pitot-static energy than the anti-hairpin maneuver. The geometric energy losses for pilot 3 matched with the expectations of Dynamic Soaring theory. It should be noted that the geometric energy includes the motion of the air mass while the Pitot-static derived energy is calculated relative to the motion of the air mass. This may somehow account for why the geometric energy losses match Dynamic Soaring theory while the Pitot-static losses do not match the theory for pilot 3.

As seen in the figures in Appendix I: Plots of Energy Height Lost Using the Averaging Method, on average the hairpin maneuver resulted in less energy loss (both Pitot-static and geometric) than the anti-hairpin maneuver for all three entry airspeeds. The no shear energy loss was typically greater than the hairpin maneuver and less than the anti-hairpin maneuver on average.

Representative plots of how the energy height varied throughout the maneuvers are shown in Appendix H: Energy Height Plot Description.

The Existence of Dynamic Soaring for full size sailplanes

The results shown in Table 1 through Table 3 revealed the following: typically performing the hairpin maneuver in wind shear resulted in less energy lost than when performing the anti-hairpin maneuver in wind shear or the DS FTT in no shear. The differences in the final total energy states were directly related to the presence of horizontal wind shear. This provided proof of concept that Dynamic Soaring did exist for a full size sailplane.

Using design of experiments, a general linear model analysis yielded a model for the Pitot-static specific energy loss that was highly dependent on three variables and the mean value of the energy loss. Two forms of the energy height model were discovered depending upon the pilot flying the maneuver:

$$E_{s_{P-s}} = -160.2\text{ft} + 8.6 \frac{\text{ft}}{\text{pilot}} (P_{2,3}) + 557.3 \frac{\text{sec}}{\text{ft}} (WS) - 3.8 \frac{\text{ft}}{\text{knot}} (AS - 95) - 0.09 \frac{\text{ft}^2}{\text{knot}^2} (AS - 95)^2$$

or

$$E_{s_{P-s}} = -160.2\text{ft} - 16.1 \frac{\text{ft}}{\text{pilot}} (P_1) + 557.3 \frac{\text{sec}}{\text{ft}} (WS) - 3.8 \frac{\text{ft}}{\text{knot}} (AS - 95) - 0.09 \frac{\text{ft}^2}{\text{knot}^2} (AS - 95)^2$$

In the model P_x represents pilots 2 and 3, or pilot 1, WS represents the wind shear in $\frac{\text{ft/sec}}{\text{ft}}$ (negative in the case of anti-hairpin maneuvers), and AS represents the maneuver entry airspeed.

The energy height model's standard deviation of the mean (standard error) is 19.7 feet. This standard deviation was significant because it demonstrated that 95 percent of the collected data was within ± 40 energy height feet of the energy height model's mean. The test had 99.9 percent power to detect any differences greater than 10 energy height feet. So, it can be stated that there is a linear dependence of energy loss on the wind shear or stated more simply; the sailplane extracted energy from the wind shear. The DOE analysis showed greater than 99.9 percent confidence that energy loss was related to wind shear. For further DOE explanation see Appendix C: Design of Experiments Analysis.

Comparison with the AFIT model

A MATLAB® model of the L-23 sailplane was developed using drag polar data obtained from the SENIOR IDS test management project and the stability derivatives and moments of inertia information obtained from the HAVE BLADDER test management project. This information was developed into a full six degree of freedom flight simulation at the NASA DFRC simulator facility in order for the test team to refine the DS FTT and to develop energy state predictions based on anticipated wind shear conditions in the test area. A linear wind shear model was used based off of historical wind shear data at Edwards AFB dating back to April 1997. Wind shear strength was varied between 0.01/sec to 0.03/sec based off of this data. Overall, the MATLAB® L-23 flight simulator was satisfactory as a Dynamic Soaring research tool.

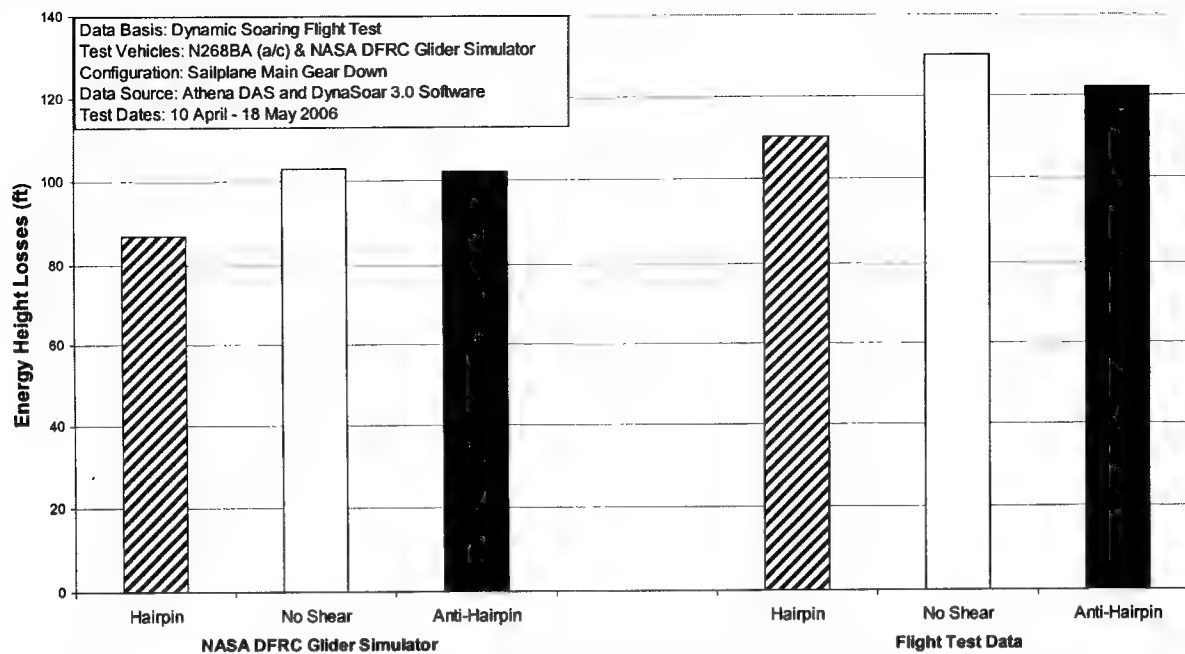


Figure 6: 85 Knot Entry Speed Glider Simulator and Flight Test Comparison (Pilot 1)

A total of 24 flight simulator runs by pilot 1 were documented and used as a comparison to actual flight data. For the 85 KIAS maneuvers, the NASA glider simulator predicted less energy loss, on the order of 20-27 energy height feet, than was actually experienced. But, the overall trend of the simulator data matched reality very closely as shown in Figure 6.

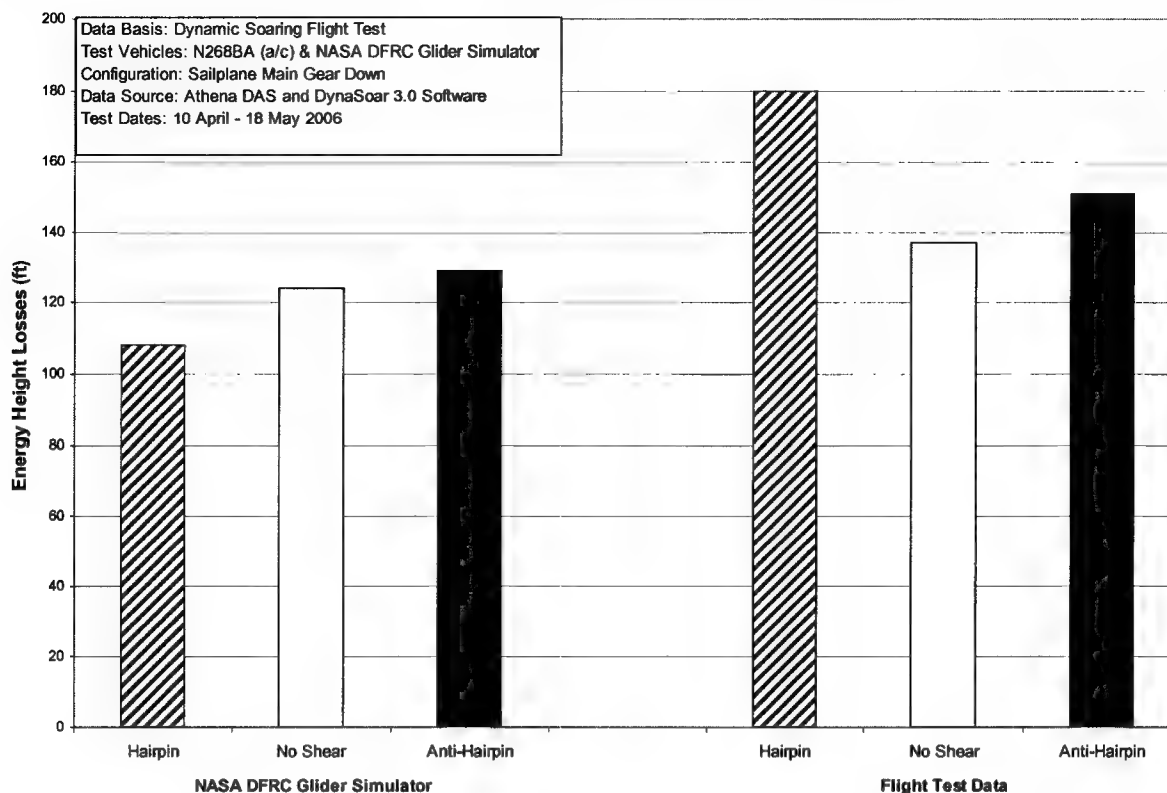


Figure 7: 95 Knot Entry Speed Glider Simulator and Flight Test Comparison (Pilot 1)

Figure 7 shows that the hairpin maneuver simulator data for pilot 1 did not match the flight test data at 95 KIAS. The no shear and anti-hairpin simulator data match the trends of the flight test data for these maneuvers although the simulator predicted less energy loss than the flight test data showed as previously discussed. The flight test data for pilot 1 at this condition contains anomalies speculated to be due to small sample size, and did not agree with Dynamic Soaring theory.

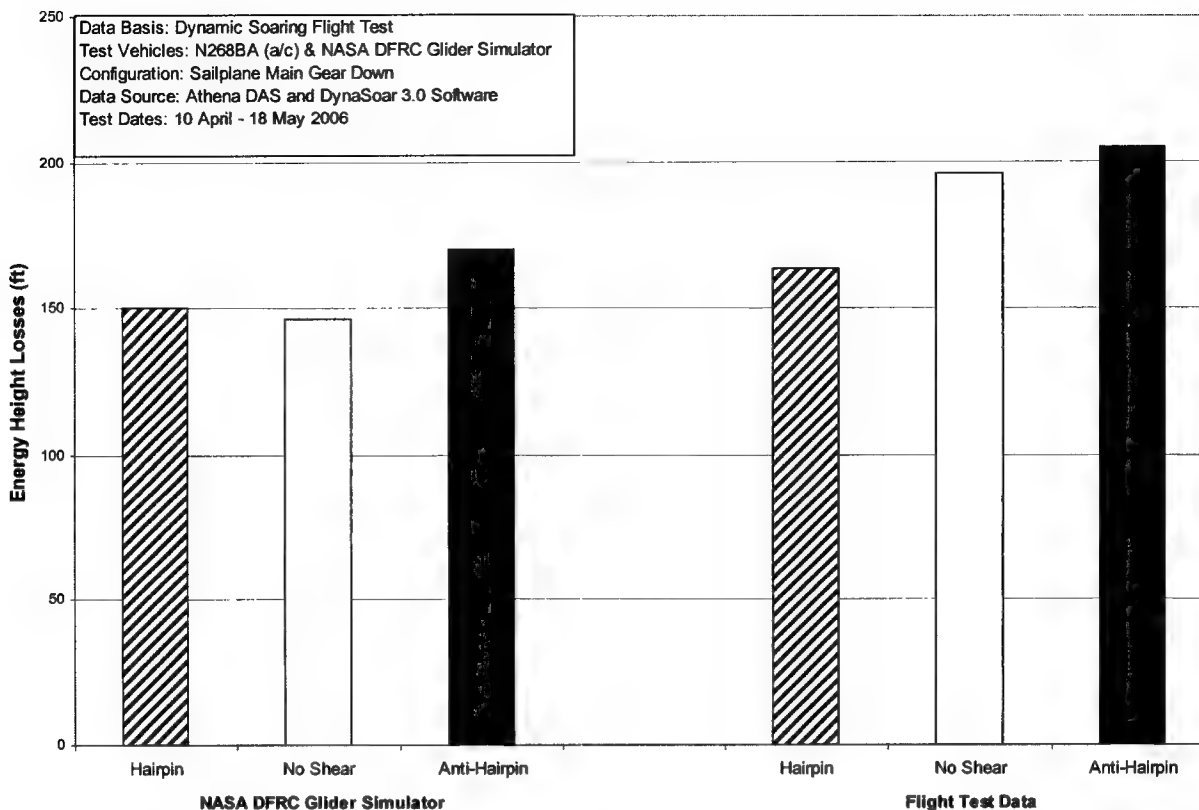


Figure 8: 105 Knot Entry Speed Glider Simulator and Flight Test Comparison (Pilot 1)

For the 105 KIAS entry condition, a similar energy height loss was noted between the simulator and actual flight for the hairpin and anti-hairpin maneuvers. In the no wind shear condition, the simulator data showed less energy loss than predicted by Dynamic Soaring theory. This caused the difference between flight test data and simulator data with no shear to be larger than the difference in energy lost shown at the other conditions.

Overall, the test team found the use of the NASA DFRC simulator and MATLAB[®] model to be invaluable in studying Dynamic Soaring. The model assumed a more optimistic drag polar than what the sailplane actually produced, and this fact accounted for the consistent smaller energy height losses of the simulator compared to flight test. The drag polars produced by a previous TPS TMP's flight test data were collected for trimmed flight conditions with negligible aileron and rudder deflections. However, during the DS FTT maneuver the ailerons and rudder were continuously deflected leading to more drag than in the trimmed flight condition. Additionally, the wind shear used in the simulator was linear with respect to altitude and was known exactly. However, the wind shear in the real world was not always linear, and was not known with the same accuracy. These two factors accounted for most of the differences between the flight test data and the simulator data.

Employment by glider pilots

The Dynamic Soaring maneuver was evaluated from both a handling qualities and practical employment standpoint. Overall from a handling qualities perspective, the maneuver was relatively easy to fly compared to the standard glider maneuvers (i.e. steep turns, slow flight, etc) that a typical soaring pilot would execute. On average, a 2.0 g pull was used to initiate the DS FTT maneuvers at the 95 and 105 KIAS points and 1.5-1.8 g on the 85 KIAS points. The stick and rudder forces and deflections during the maneuver were not objectionable. At no time during the test flights was safe aircraft control in question.

Normal altitude gained during the maneuver ranged from 300-400 feet during the 105 KIAS points to 150-200 feet during the 85 KIAS points. During the test program, several data points were flown at 200 feet AGL and 105 KIAS. Although workload slightly increased at the lower altitudes due to ground rush, performance standards did not suffer and desired performance was still attained. Likewise, control forces and deflections as well as aircraft controllability was never in question at these lower altitudes.

The difficulty of the maneuver to fly was assigned a Cooper-Harper rating based off of the following criteria:

Desired: Maintain pitch and bank to within ± 5 degrees of entry, peak, and exit parameters as discussed earlier in the test procedures section. Airspeed must have been maintained within ± 5 knots of entry and peak airspeed parameters. At the conclusion of the maneuver, the pilot must have rolled out within ± 10 degrees of the initial heading.

Adequate: Maintain pitch and bank to within ± 10 degrees of entry, peak, and exit parameters as discussed earlier in the test procedures section. Airspeed must have been maintained within -5 to +10 knots of entry and peak airspeed parameters. At the conclusion of the maneuver, the pilot must have rolled out within ± 20 degrees of the initial heading.

Figure 9 illustrates the Cooper-Harper Ratings for each test pilot on the test team. The project pilots had diverse flying backgrounds, but the Cooper-Harper Ratings were similar among all the pilots. Pilot 1 was a C-130E pilot, pilot 2 was an F-15C pilot with a commercial sailplane license, and pilot 3 was an AV-8B pilot. Pilots 1 and 3 had no previous glider experience. On average, a Level II Cooper Harper rating was assigned. (See Appendix J: Cooper-Harper Rating Scale.) Desired performance was achieved by each team member. However, moderate pilot compensation was required to attain desired performance because of the required precision of the maneuver. Overall, the DS FTT was executed with tolerable pilot workload primarily due to the advanced avionics and maneuver quality assistance provided by the flight test engineers (FTE) and the flight test navigator (FTN) from the rear cockpit. During the maneuver the FTE/N would call the altitude change from start altitude so the pilot could remove it from his cross check. In addition, the FTE/N was the primary safety monitor for terminating the maneuver due to a low energy state or descending through minimum altitudes during DS FTT maneuvers.

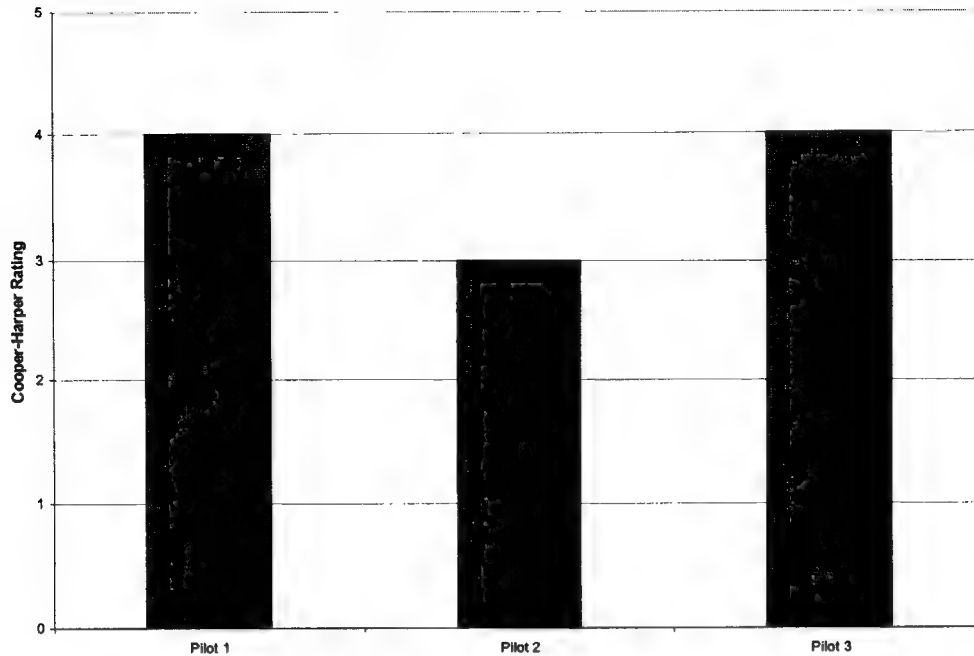


Figure 9: Cooper-Harper Ratings

Overall, the ability to extract energy from horizontal wind shear did exist. However, the data also indicated that the energy gained was relatively small. During the test window, relatively light wind shear profiles were generated by the light temperature inversion and boundary layer effects experienced in the flight test area. The strongest wind shear encountered during the test window equated to an increase of 2.5 knots per 100 feet. Hence, little energy was available to extract from the wind shear. Although more difficult to map precisely, stronger wind shears can be generated when the wind is partially blocked by an obstacle. This situation exists on the leeward side of mountain ridges and might provide the best opportunity to experience Dynamic Soaring. **Conduct Dynamic Soaring tests in the stronger wind shears generated by orthographic features. (R1)¹**

In addition, the L-23 drag penalties incurred due to aircraft design possibly outweighed much of the energy benefit gained during the hairpin maneuvers. The test aircraft L-23 suffered from high parasite drag due to the fixed landing gear, metal rivet construction, and imperfections in the fit of major components (canopy, flight control surfaces, etc). Typical competition sailplanes feature modern glass composite construction and sleek low drag designs. Gaps between canopies and flight control surfaces are typically sealed with tape in order to present a seamless surface to the wind. As a result, competition sailplanes can have lift to drag ratios in excess of 60:1 vice the 24:1 glide ratio of the test aircraft. As a result, low drag sailplanes are better suited for extracting energy via Dynamic Soaring techniques. A high performance glider, with lower drag, and increased maneuverability, would possibly see an enhanced positive net effect from the Dynamic Soaring maneuvers in wind shear. **Conduct Dynamic Soaring tests in high performance sailplanes. (R2)**

¹ Numerals preceded by an R within parentheses at the end of a sentence correspond to the recommendation numbers tabulated in the Conclusions and Recommendations section of this report.

The avionics, instrumentation included in the glider, and weather support for the test flights were invaluable in order to fly accurate maneuvers. The attitude display allowed for accurate and repeatable maneuvers in pitch and roll. In addition, the airspeed and altitude readouts were clear and sensible. Likewise, the GPS moving map display coupled with the hands on stick (HOS) activated ground track symbology maximized the precision to which the DS FTT maneuvers could be flown. These avionics were unique to this aircraft and would not be present in a typical production sailplane. Furthermore, atmospheric data were collected using dedicated weather balloons and mobile SODAR. A typical sailplane pilot would not have access to these resources to accurately map the atmosphere around the sailplane. Strong shears can be felt on tow in the form of turbulence, and temperature inversions can be indicated by low haze or drifting columns of smoke or dust. However, these indications are ultimately only an approximation made by the pilot in the cockpit real time. Hence, maneuver precision and energy extraction from wind shear would suffer in a production sailplane with a typical soaring pilot.

The Dynamic Soaring maneuver was not difficult to fly given the special instrumentation and crew coordination employed during SENIOR ShWOOPIN flight testing. However, Level II ratings were assigned due to the precision required in order to standardize data collection. Dynamic Soaring theory indicates that it is possible to extract energy from horizontal wind shear using maneuvers other than the DS FTT used for this project. These maneuvers may require less precision in order to be performed and may be able to be executed with a standard sailplane's instrumentation. **Investigate alternate Dynamic Soaring maneuvers that require less precision and instrumentation. (R3)**

Finally, the data indicated that the Dynamic Soaring maneuver was more beneficial at the high speed points from 95-105 KIAS. In order to obtain these entry speeds in the L-23 from a start airspeed of 60 KIAS, 700-800 feet of altitude were lost during the dive. This is not a realistic profile for a pilot who is trying to maximize glider energy state because it involved sacrificing tremendous altitude. Since precise wind shear data would not be known, this dive might ultimately result in a loss of energy that may not be recovered. Hence, from an energy height standpoint, hairpin maneuvers in uncertain atmospheric conditions would be risky for a soaring pilot to perform.

In summary, the Dynamic Soaring maneuver was a relatively mild maneuver that was easy to fly, but the precision required for flight test data collection increased the workload significantly. Valid data were collected throughout testing that proved the theory of Dynamic Soaring. However, in a production sailplane that lacks specialized instrumentation and detailed atmospheric data, the risk to a sailplane's energy state by performing Dynamic Soaring maneuvers may be outweighed by the energy benefits gained by basic Static Soaring techniques, such as thermal, ridge lift, etc.

Conclusions and Recommendations

SENIOR ShWOOPIN represented the first documented study into the applicability of Dynamic Soaring for full size sailplanes. All test points in the program were flown and all objectives were met. Overall, this project proved that full size sailplanes could extract energy from horizontal wind shears. Recommendations for future studies are provided below in order of priority.

Although this project successfully proved the theory of Dynamic Soaring for full size sailplanes, the amount of energy benefit was relatively small. The strongest wind shear encountered during this test program equated to a 2.5 knot increase per 100 feet of altitude gain. Hence, little energy was available to extract from the wind shear. It is very likely that stronger wind shears than those encountered during this test program could be generated by flying on the leeward side of mountain ridges when the winds are perpendicular to the ridge line. Although these wind shear profiles would be harder to map due to the complexity of the flow fields, this scenario represents the best opportunity to experience suitable Dynamic Soaring conditions.

Conduct Dynamic Soaring tests in the stronger wind shears generated by orthographic features (R1, page 17).

Furthermore, the low aerodynamic performance of the L-23 sailplane mitigated much of the energy gain realized by flying the hairpin maneuvers in the light wind shears present during the test window. Data analysis and a comparison of the flight test and simulator data indicated that more energy could be extracted from the atmosphere with stronger wind shears and low drag profile sailplanes. Data analysis further indicated that faster entry speeds were ideal for Dynamic Soaring since this allowed the sailplane to penetrate higher through the wind shear. At these higher speeds, however, parasite drag dominates the performance of the L-23 sailplane.

Conduct Dynamic Soaring tests in high performance sailplanes. (R2, page 17)

Because of the ground breaking nature of this flight research and the limitations of the environment and sailplane described above, accurate knowledge of atmospheric wind shear conditions and precise control of the Dynamic Soaring maneuvers were critical. Such precision was required in order to best position the sailplane to take advantage of the wind shear and to ensure the repeatability of the maneuvers. This required advanced custom built avionics and dedicated weather monitoring support. The required precision generated additional workload for the aircrew since they had to constantly monitor the position and strength of the wind shears and use the electronic displays to track the sailplane's attitude and flight condition within tight tolerances through the Dynamic Soaring flight test technique. Since this project proved the basic existence of Dynamic Soaring for full size sailplanes, future research should expand the practical knowledge base of this technique by discovering maneuvers that require less instrumentation and precision to successfully extract energy from horizontal wind shears. Maneuvers of this type would be much easier for a typical soaring pilot to perform in a sailplane equipped with standard avionics.

Investigate alternate Dynamic Soaring maneuvers that require less precision and instrumentation. (R3, page 18)

Finally, the MATLAB[®] flight simulator model was an excellent research tool to study the effects of Dynamic Soaring in various wind shears. The model, however, featured a non-maneuvering drag polar. Although the energy height results of the simulator flights closely matched the basic trends of flight data, the simulator's energy losses were consistently less than flight test energy losses. Essentially, the flight simulator predicted better Dynamic Soaring performance than what was attained by the L-23.

In conclusion, this project proved the existence of the Dynamic Soaring phenomenon for full size sailplanes. This was demonstrated by the linear dependence of the energy loss of the sailplane upon the strength of the wind shear. Future Dynamic Soaring research should focus on high performance sailplanes in stronger wind shears, which may produce significant energy savings that could be used to sustain flight.

References

1. Borrer, Sean, Major, *USAF, USAF TPS L-23 Super Blanik Drag Polar and Preliminary Investigation of Dynamic Soaring*, USAF TPS-TIM-04-04, Air Force Flight Test Center, Edwards AFB, California, September 2004.
2. Aviv, Yam-Shahor, Major, *IAF, USAF TPS L-23 Super Blanik Aerodynamic Determination, Evaluation, and Reporting Program*, USAF TPS-TIM-05-08, Air Force Flight Test Center, Edwards AFB, California, December 2005.

This page intentionally left blank.

Appendix A: Instrumentation and Displays

Sensors

The instrumentation system installed on the L-23 consisted of an Inertial Measurement Unit (IMU), an air data probe and transducers, control surface position transducers, analog-to-digital converter, a temperature probe and two tablet PC displays. The IMU and analog-to-digital converter were mounted on an adjustable plate and aligned with the centerline of the aircraft. The centerline was defined by the rib running along the top surface of the aft fuselage. The plate was then tilted to align it with the aircraft fuselage reference line. The fuselage reference line was defined by two marks on the side of the glider at the forward and aft ends. The plate was tilted left and right to align with the leading edge of the wing. Finally, a laser sight was used to align the air data probe with the fuselage reference line and center it along the aircraft centerline. All angular measurements were therefore referenced to a body axis coordinate system whose x-axis was aligned with the fuselage reference line and a y-axis aligned with the wing leading edge at the root.

Guidestar GS-111m

An Athena Controls Guidestar 111m (GS-111m) inertial measurement unit (IMU) served as the central component in the instrumentation system. The GS-111m used accelerometers, angular rate sensors, GPS, and a magnetometer to compute a full inertial attitude solution. Pitot-static pressures from a nose-mounted 5-hole probe were measured by the GS-111m to determine airspeed, altitude, angle-of-attack (AOA), and angle-of-sideslip (AOS). Pressure transducers on the TPS GS-111m had a dynamic range of $\pm 26,221.9$ Pascals for AOA and AOS, and 16,596 Pascals for dynamic pressure. Total air temperature was measured by a resistive temperature detector (RTD) mounted under the right wing. The RTD voltage was sampled by a 14 bit analog-to-digital input on the GS-111m. Data were sampled and written to a 32 Megabyte onboard memory chip for post-flight download. The GS-111m updated its navigation solution at 50 Hertz. The data sampling rate was software selectable with currently available rates of either 25 Hertz or 50 Hertz. The 50 Hertz sampling rate was used for this program. The GS-111m was modified to accept a digital signal from an analog-to-digital converter that was wired to the position transducers. This hardware modification consisted of a circuit board housed in a generic black box that could be mounted anywhere in the proximity of the GS-111m and connected to the GS-111m using an RS-232 serial cable. The interface control document can be obtained from Athena Controls. A full description of the GS-111m can be obtained by contacting Athena Controls.

Air Data Probe

An air data probe purchased from Computer Instruments Corporation was used to measure static pressure, total pressure, AOA, and AOS. The initial design called for a constant 0.75 inch outer diameter probe. This was modified by increasing the diameter of the aft end up to 1.25 inches to provide sufficient wall thickness for attachment to the boom. The AOA and AOS measurements were made using a pressure differential, total pressure, and a scale factor. The probe had a scale factor of 4.526366 1/radian. During a previous project the air data probe was calibrated using a trailing cone (reference 1).

Resistive Temperature Detector

The RTD purchased from Computer Instruments Corporation was used to measure total temperature. The platinum RTD had a nominal resistance of 500 Ohm and a scale factor of 0.00385 Ohms/Ohm/degrees C. The RTD was powered by an Action Instruments Ultra Slimpak G418-0001. A full description of this device may be obtained by contacting Computer Instruments Corporation. The output voltage of the RTD was sampled by a 14 bit analog-to-digital converter on the

GS-111m. During a previous project an ice bath calibration of the RTD connected to the GS-111m resulted in the following relationship between RTD resistance and measured voltage:

$$R_{_RTD} = 474.0085 \text{ Ohm} + 61.6398 \text{ Ohm/volt} * \text{Voltage}$$

A platinum RTD had a sensitivity curve with a slope of 0.00385 Ohms/Ohm/degrees C over the temp range [-10 +50] degrees C. This gave a relationship between RTD resistance and temperature:

$$T(^{\circ}\text{C}) = -257.3989 \text{ C} + 0.5148 \text{ C/Ohm} * R_{_RTD}$$

Combining these equations gives a relationship between voltage measured by the IMU and total air temperature:

$$T(^{\circ}\text{C}) = (0.5148 * (474.0085 + (\text{Voltage} * 61.6398))) - 257.3989$$

Surface Position Transducers

String potentiometers (5K Ohm) made by Space Age Technologies were mounted to measure control surface deflections of the elevator, rudder, left and right aileron and elevator trim tab cable. The potentiometers were mounted in front of the surfaces and connected to the surface with a steel cable. Wiring to the potentiometers was run internally from the DAS pallet to the mounting point for the potentiometer. During a previous project calibration curves were created using a digital inclinometer to measure the angle of the control surface and plot it versus the voltage output for the elevator, ailerons and trim tab. Calibration of the rudder was accomplished by finding the center of rotation on the top of the rudder. A protractor was then placed above this point and deflection angles were read using the seam of the rudder that described the left-right plane of symmetry. All control surface calibration curves were linear.

GS-111m Interface

Interface to the GS-111m was made via five serial ports accessible through 51 pin connectors. Each serial port was configured for RS-232 communication at 115.2 Kilobits/second. The slow data rate was chosen primarily to ensure reliable communication with the Motion Computing tablet PC used for cockpit data display. Operationally, only ports 1-3 were used.

Laptop PC Interface

Serial port 1 was used to interface with a laptop PC for IMU initialization. After applying power to the IMU, an Athena Graphical User Interface (GUI) was used to set internal IMU parameters and switch the IMU into the Air Mode. After initialization, the laptop was disconnected prior to flight.

Tablet PC

Serial port 2 was used to communicate with a Motion Computing tablet PC. The tablet PC displayed flight parameters in the cockpit (see Figure A-1) and had the capability to start and stop data logging via a HOS controls. The tablet PC in the front cockpit was connected to the GS-111m using a serial to USB connector cable. Data from the tablet PC in the front cockpit were passed to the tablet PC in the rear cockpit via an ethernet cable.

Point-to-Point Protocol Terminal

Serial port 3 was configured for a point-to-point protocol (PPP) connection to a PC. The port speed was set by Athena Controls to be 115.2 Kilobits/second. The port was used to download test data to a laptop using WS-FTP 6.0 software. The data were transferred simply to empty the memory of the GS-111m for the next flight.

Data Acquisition

The list of parameters written to memory on the GS-111m was software programmable, but required support from Athena to perform. Reconfiguring the GS-111m could be accomplished with a simple spreadsheet based program which produced a configuration file that must be downloaded to the unit. A 50 Hertz recording rate was used. Data logged by the Guidestar was saved in time and date tagged files using the convention: INSmddhhmmssyyyy. The TPS customized data stream occupied frame 4 as listed in the serial interface spec addendum and took 128 bytes. At 50 Hertz, data frame 4 consumed 3.125 Kilobytes/second. In addition to frame 4, the following frames were stored to onboard memory: Frame 2 at 1 Hertz = 173 bytes/second, Frame 3 at 10 Hertz = 740 bytes/second, Frame 8 at 50 Hertz = 1650 bytes/second.

In addition to the data recorded on the GS-111m the tablet PC recorded data in .bin and .csv file formats. File recording was controlled using the HOS control on the stick in the front cockpit. The first time this button was pushed started recording data while simultaneously zeroing the maneuver downrange and crossrange distance and altitude. The next time the button was pushed the file was stopped and logged to the tablet PC using the following naming conventions: TPSmddyyyy hh_mm_ss.bin and TPScalcmddyyyy hh_mm_ss.csv. Because the tablet PC offered a simpler interface it was used as the primary data acquisition system, and the GS-111m was only used as a backup data source in case the tablet PC failed to record (this never happened).

Tablet PC Display

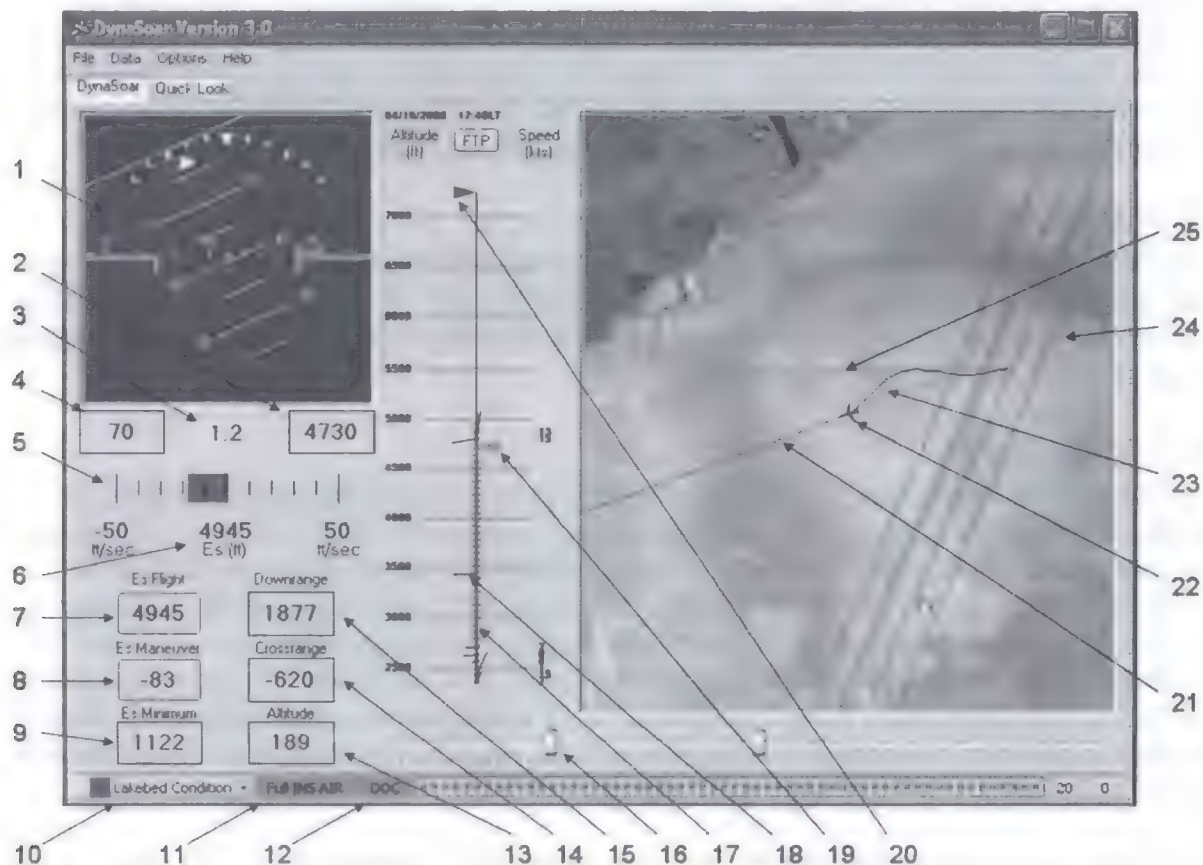


Figure A-1: Tablet PC Display

| | | | |
|----|--|----|---|
| 1 | Attitude ball with embedded heading scale and heading bug (bug was set at start of maneuver when the HOS controller was pressed) | 14 | Crossrange distance from start of maneuver (ft) |
| 2 | Pressure altitude (ft) | 15 | Downrange distance from start of maneuver (ft) |
| 3 | Normal load factor | 16 | Wind data zoom control |
| 4 | Airspeed (KIAS) | 17 | Wind data (altitude, direction, speed) |
| 5 | Energy rate gauge (ft/sec) (Negative rate displays a red bar, Positive rate displays a green bar) | 18 | Energy height bingo (ft MSL) |
| 6 | Energy height (ft MSL) | 19 | Pressure altitude (ft) |
| 7 | Energy height (ft AGL): Prior to takeoff this button was pressed to zero the energy height. (Below bingo energy the block turns red) | 20 | Energy height (ft MSL) (Energy height shown is not representative of an actual flight because the picture shown was not captured in flight.) |
| 8 | Energy difference from start of maneuver (ft) | 21 | Current heading reference line (red) |
| 9 | Energy height bingo (ft AGL) ¹ | 22 | Own ship icon |
| 10 | Lakebed status toggle (red/green) ² | 23 | Ground track history (blue) |
| 11 | EGL/GPS status display | 24 | Moving map display with zoom control |
| 12 | DAS status display (Green indicates data is recording) | 25 | Start of maneuver heading reference line (green) |
| 13 | Altitude from start of maneuver (ft) | | Red lakebed energy height bingo reference point ³ |

- ¹ The term “bingo” indicates that a return to base condition has been met. In this case, the minimum energy height needed to prepare for landing would have been reached.
- ² The term “red” lakebeds refers to lakebed conditions that are not conducive to operating the glider from the lakebeds. While “green” lakebeds indicate that the glider can be operated safely from the lakebed.
- ³ Energy height bingo reference point (red TACAN symbol) for red lakebed operations was also displayed on the moving map, but it is not in the field of view shown. This point could be set manually under the “Options” – “Energy” tab by entering a latitude and longitude in degrees. During red lakebed operations the energy height bingo was dynamically calculated by assuming a 16:1 L/D ratio to fly from the glider’s current location to the bingo reference point. This allowed the glider to reach the reference point with an energy height equal to 400 ft and 60 KIAS.

This page intentionally left blank.

Appendix B: MATLAB[®] Data Reduction Methodology

The Athena data acquisition system recorded the sailplane inertial velocities (North/East/Down), inertial positions (North Position/ East Position/Down Position), Euler rates (P/Q/R), and Euler angles ($\theta/\Phi/\psi$) through a blended GPS/INS navigation solution. A standard coordinate transformation matrix was then used to convert inertial velocities to body fixed velocities (U/V/W) assuming a flat non-rotating Earth reference frame. This assumption was valid due to the slow speed of the sailplane, and the short time frame and size of the maneuver with respect to the earth's surface. Indicated airspeed was recorded from the test Pitot-static boom via a calibrated transducer. Pitot-static and geometric energy heights were recorded on the Tablet PC via algorithms pre-programmed into the DynaSoar 3.0 software avionics package. All data was automatically logged individually per maneuver by date and time on the Tablet PC in the form of a Microsoft Excel spreadsheet and a .bin file. The .bin file was used to replay the sortie on the DynaSoar 3.0 display for post flight analysis. The excel spreadsheet was imported into MATLAB[®] and filtered through a first order low-pass Butterworth filter in order to eliminate high-frequency noise while still preserving the fidelity of the raw data. The resulting data file was then plotted and archived for analysis. An example plot set of a typical Dynamic Soaring maneuver is provided below for reference.

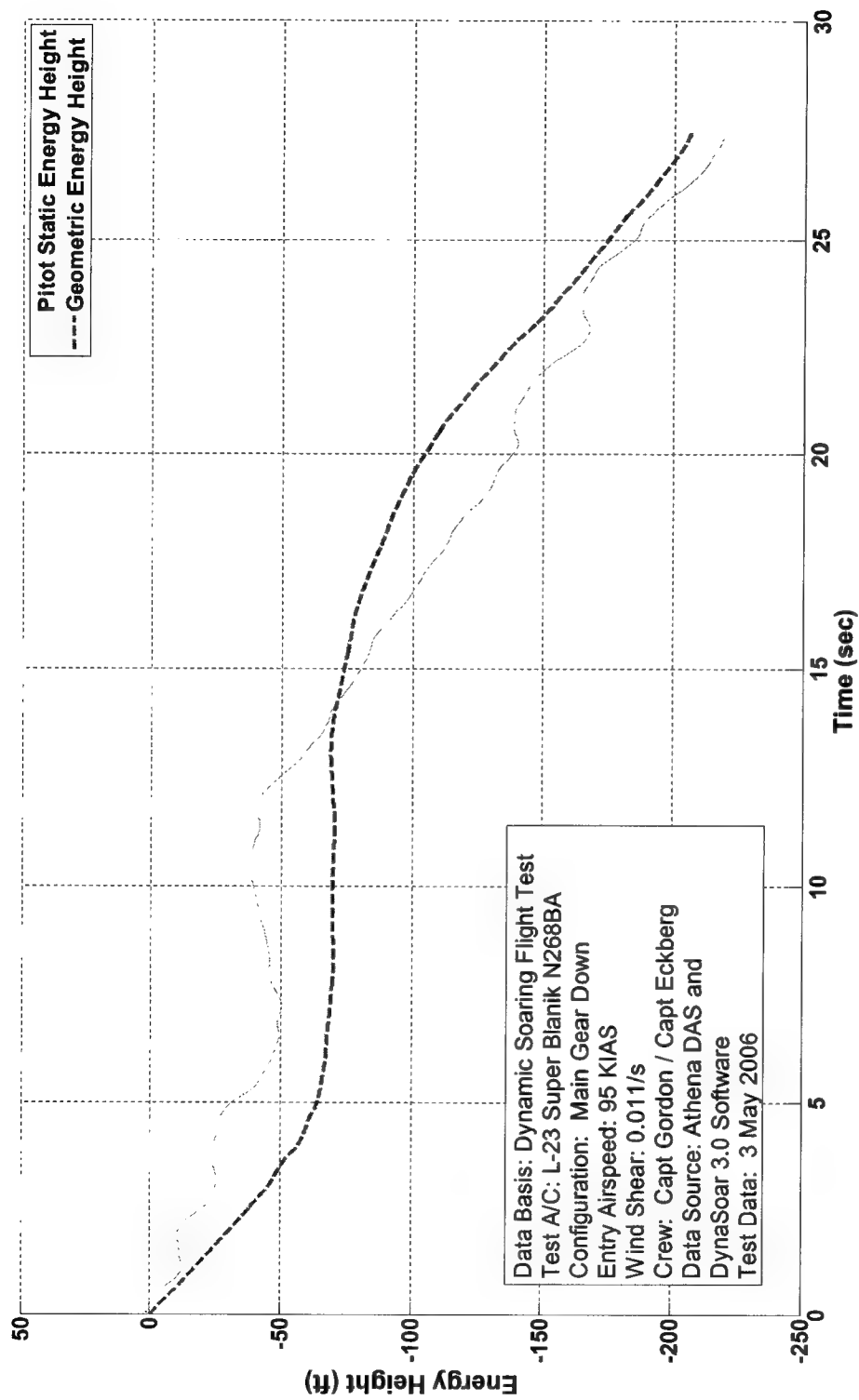


Figure B-1: Sample Plot of Pitot-static and Geometric Energy Height

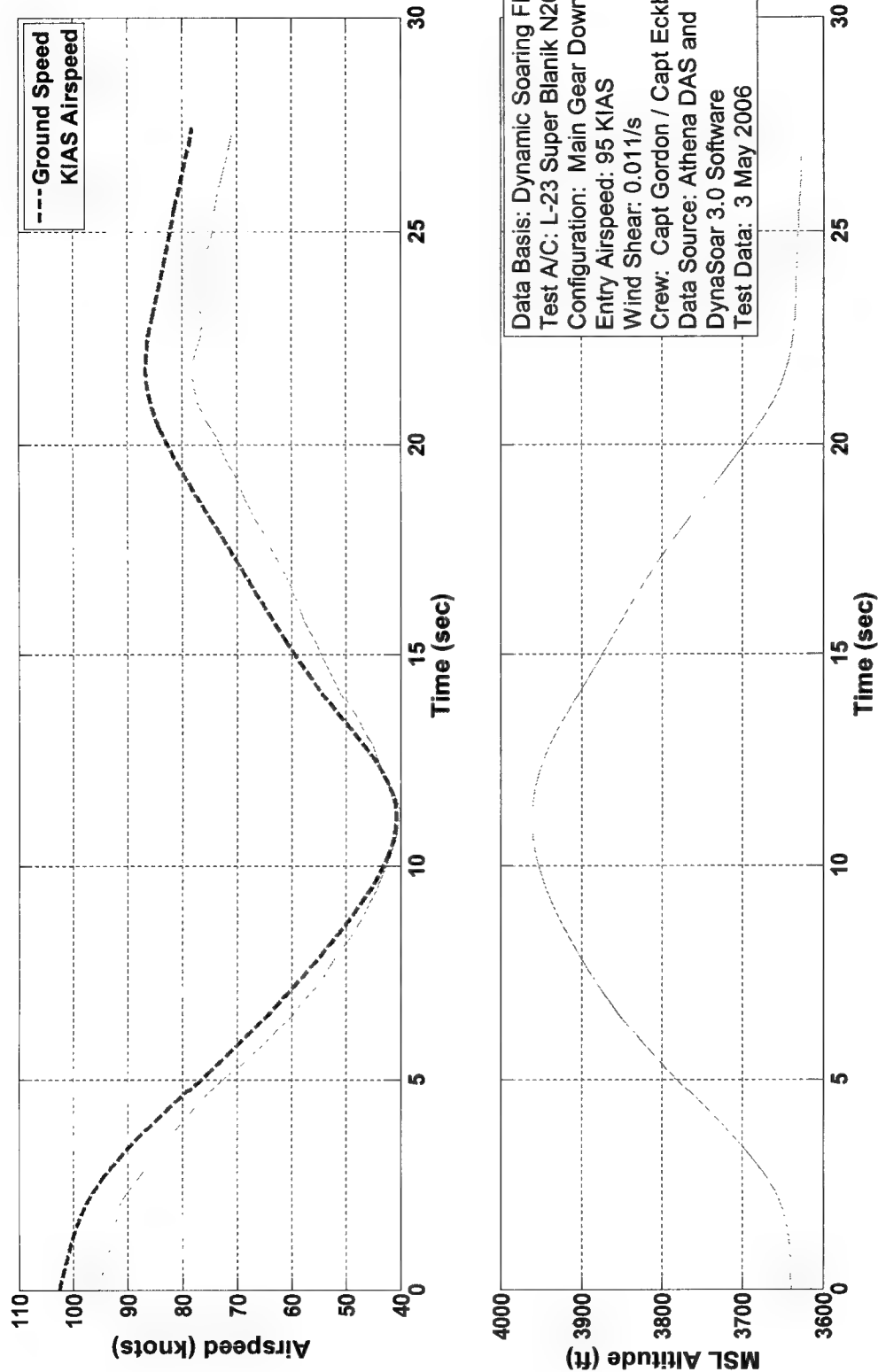


Figure B-2: Sample Plot of Indicated Airspeed, Ground Speed, and Altitude

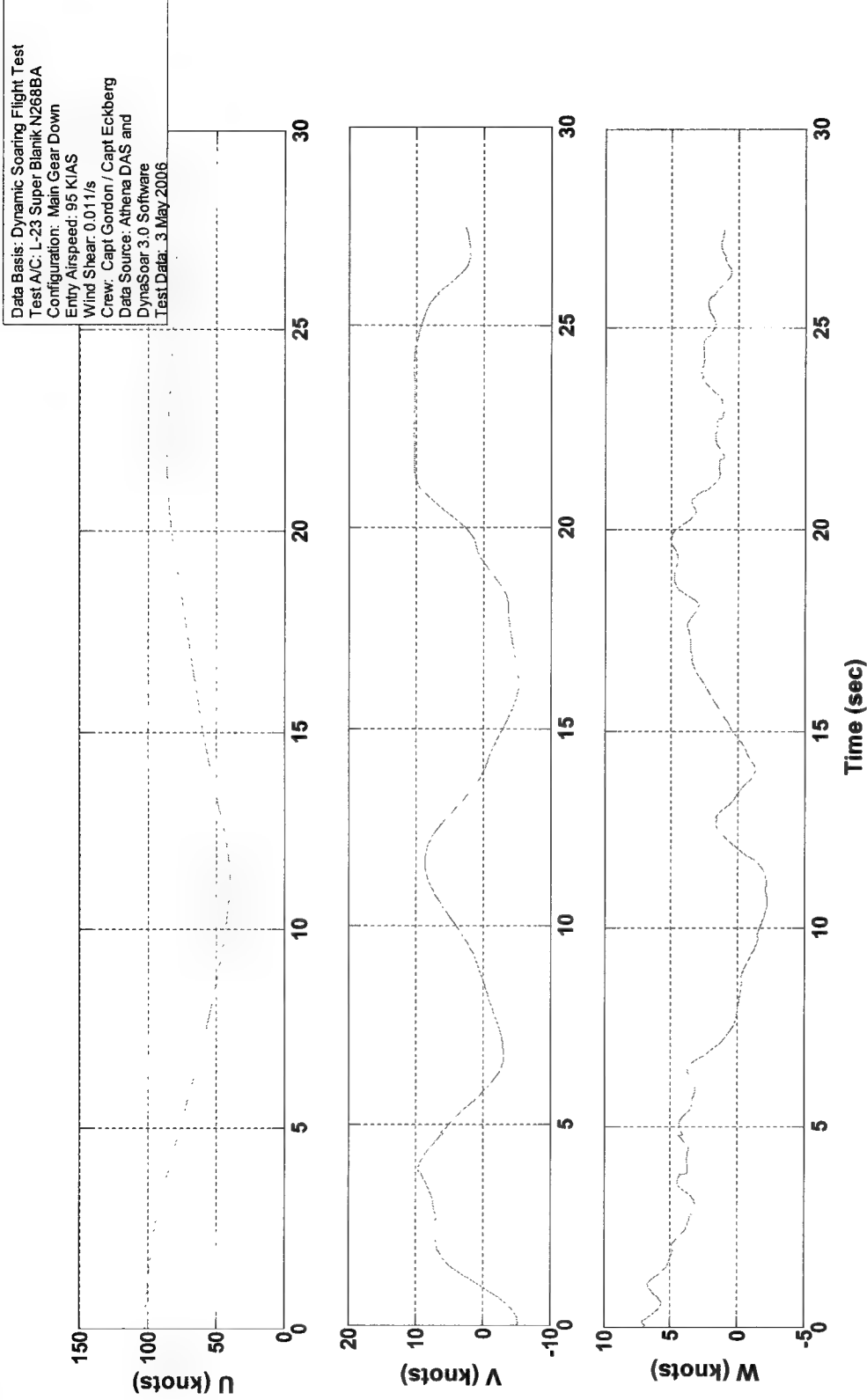


Figure B-3: Sample Plot of Body Fixed Velocities

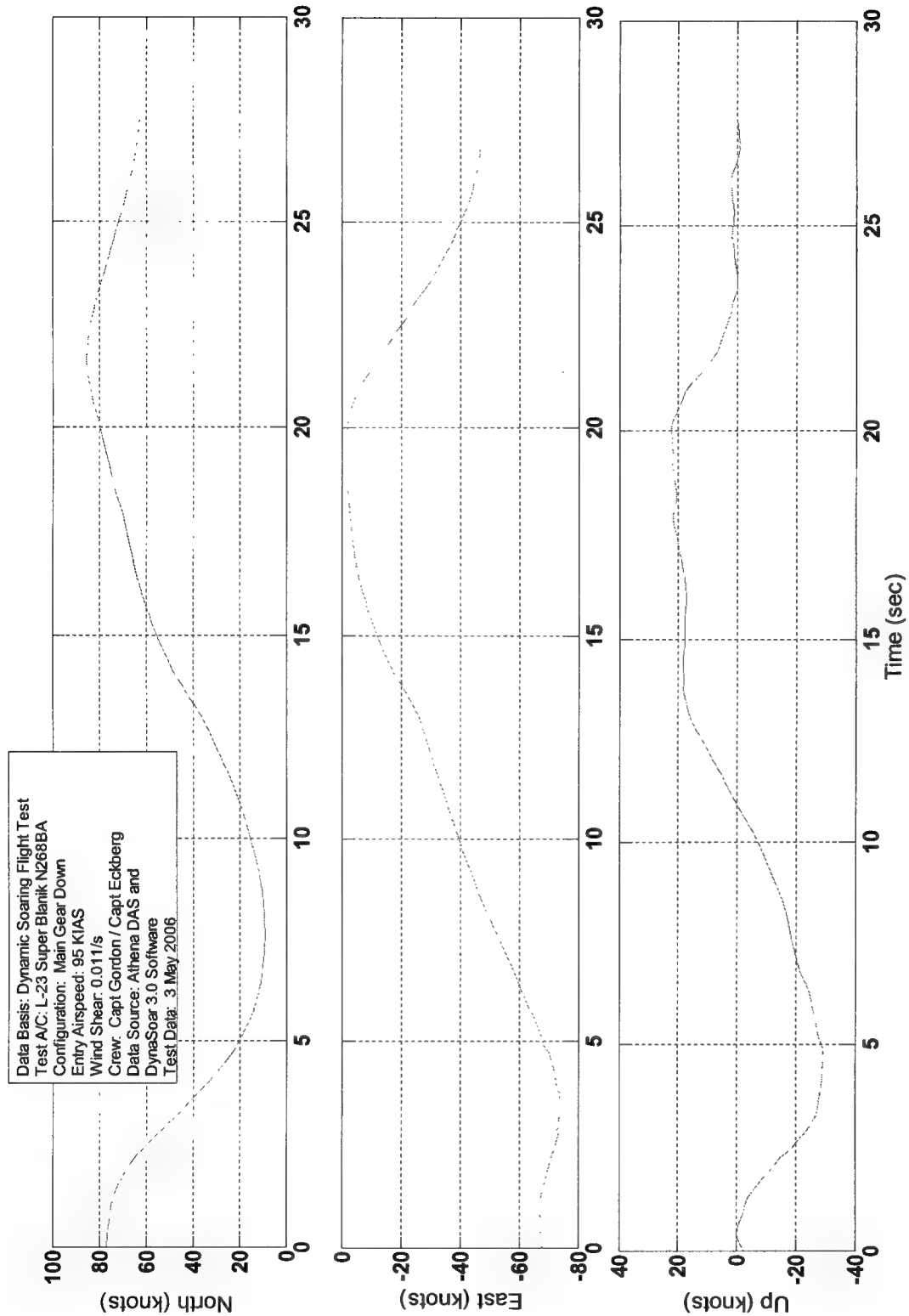


Figure B-4: Sample Plot of Inertial Velocities

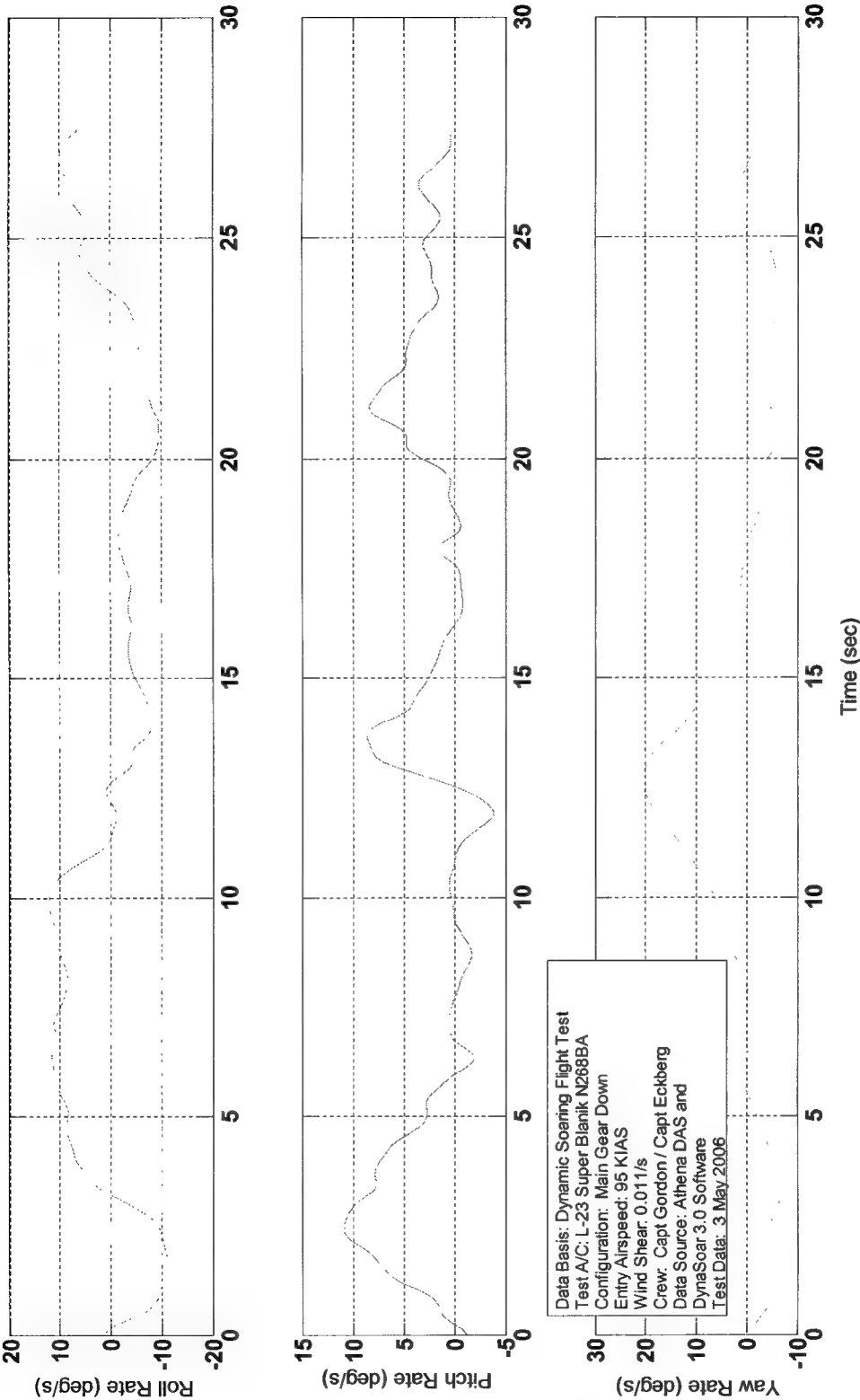


Figure B-5: Sample Plot of Euler Angle Rates

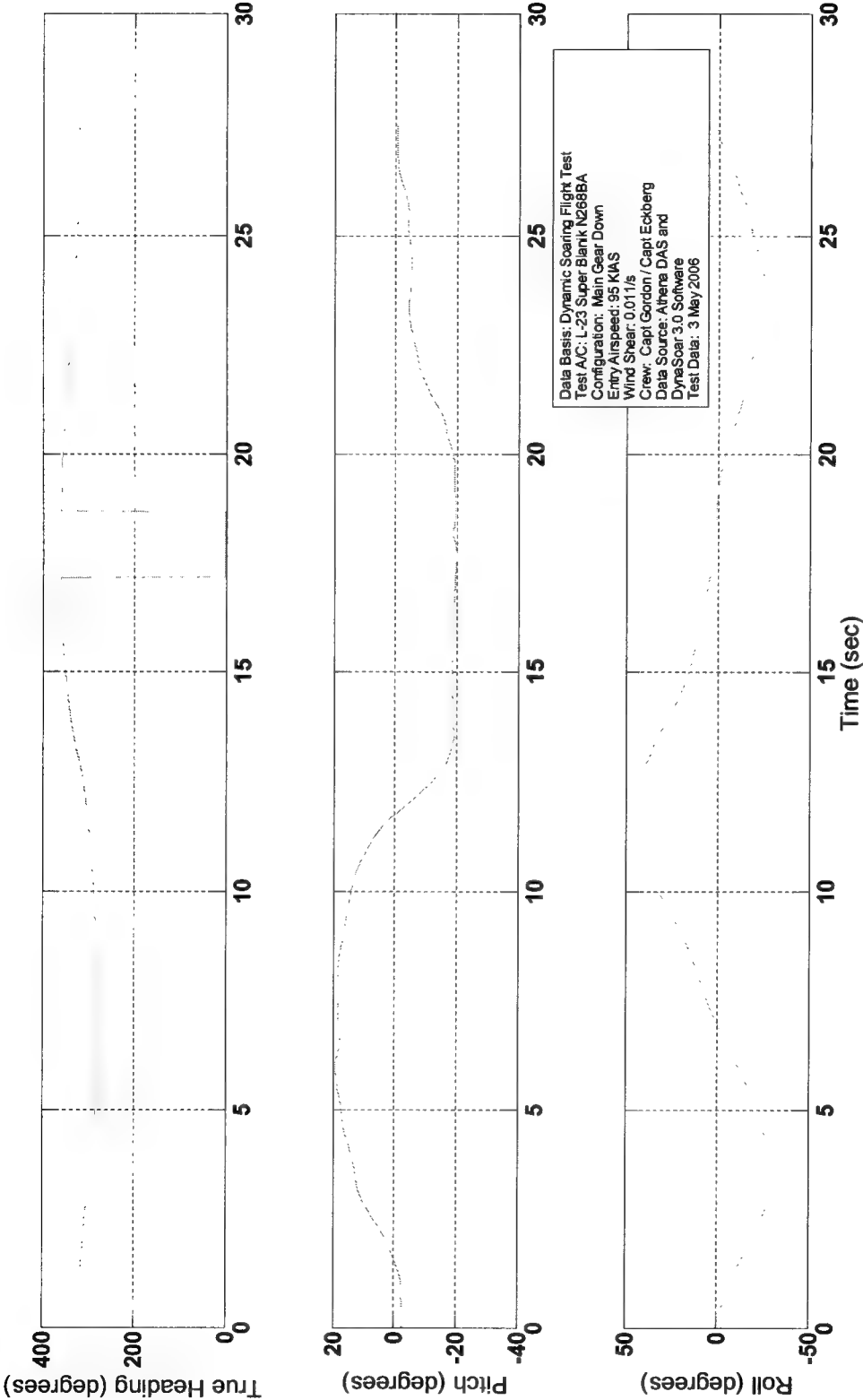


Figure B-6: Sample Plot of Euler Angles

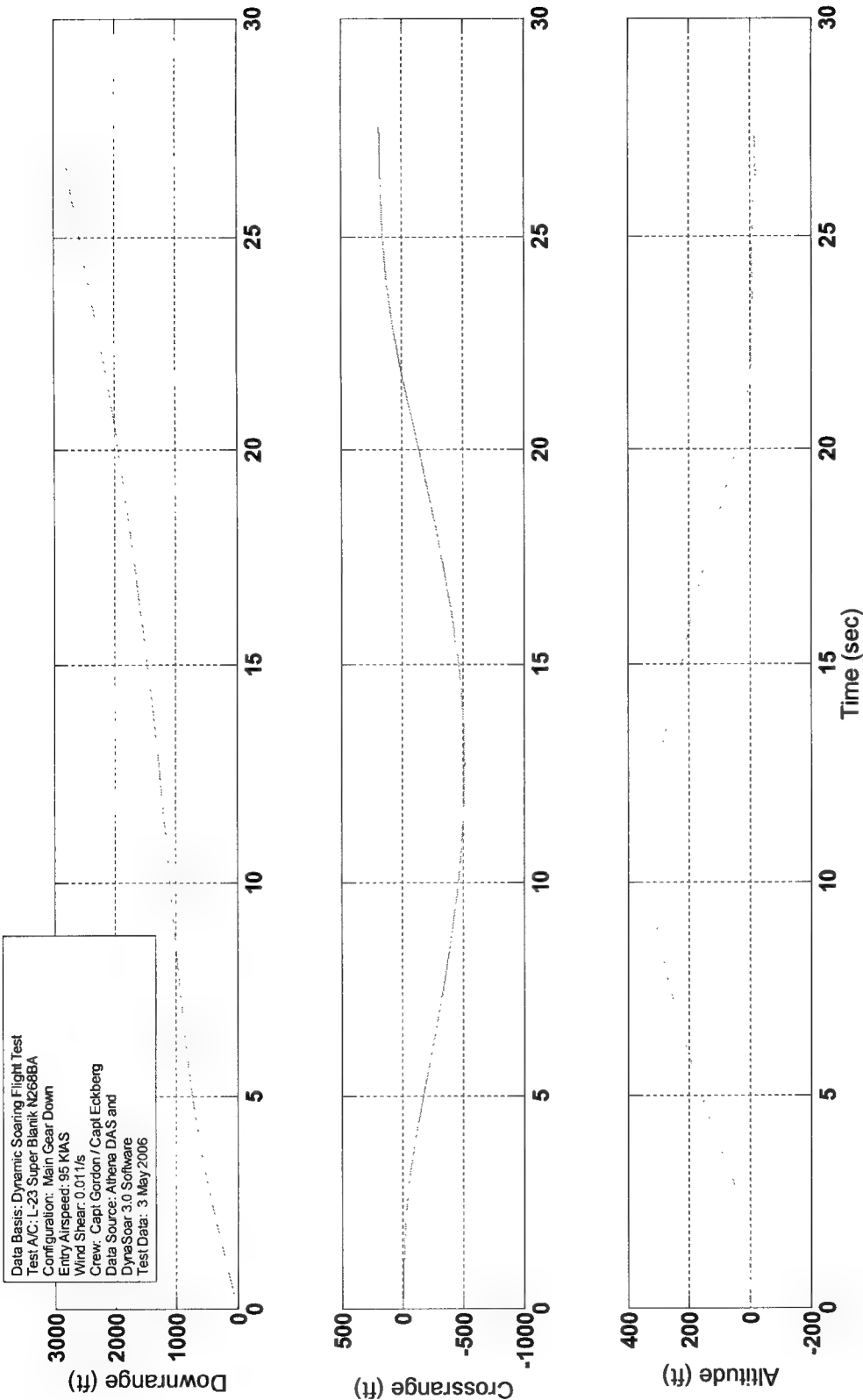


Figure B-7: Sample Plot of Inertial Position Relative to Maneuver Point

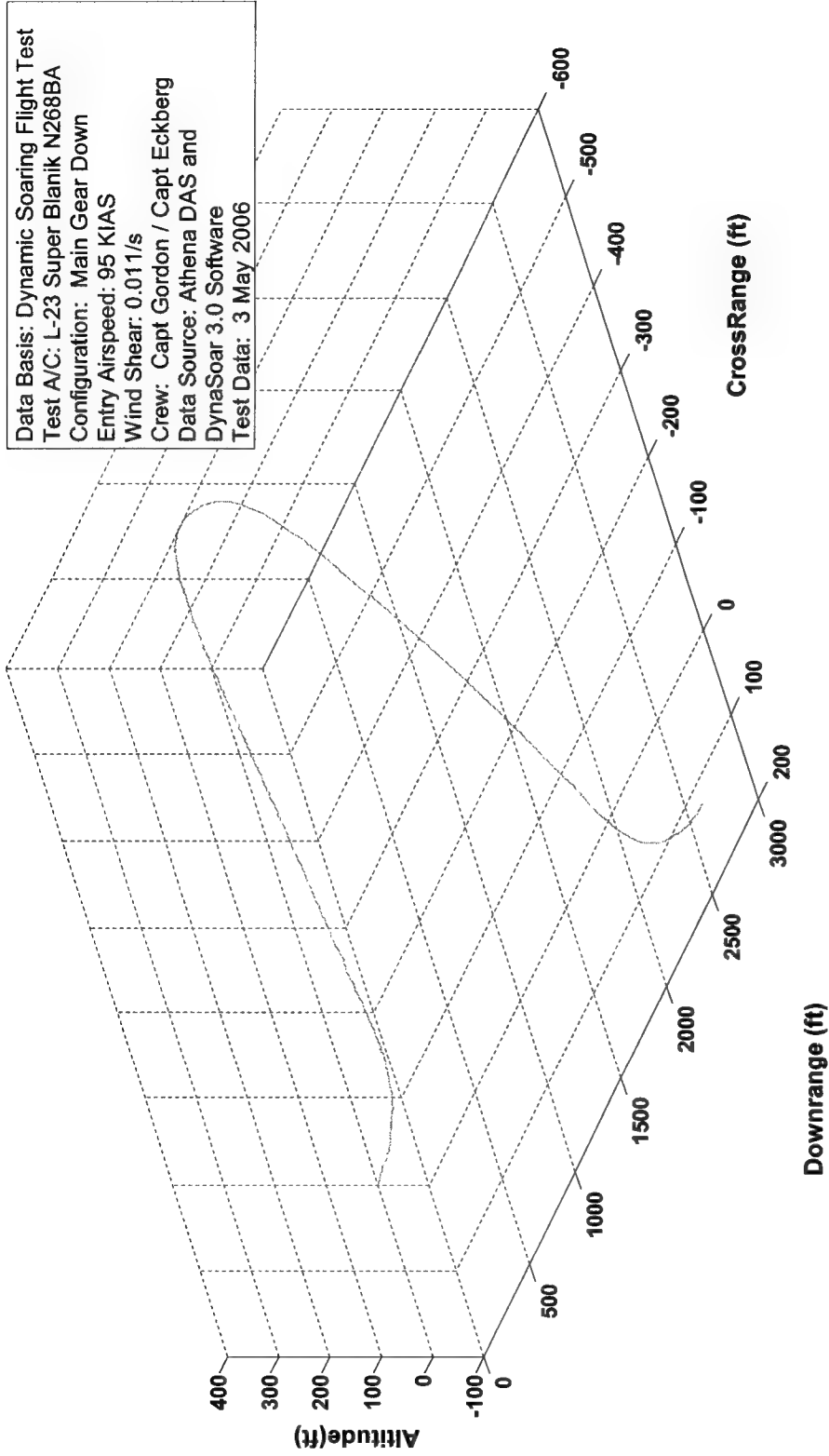


Figure B-8: Sample Plot of Sailplane Ground Track and Altitude

Appendix C: Design of Experiments Analysis

Design of experiments statistical analysis was used to determine interactions between all the controllable and uncontrollable factors. The controllable factors were pilots, entry airspeed, and maneuver type. The predominant uncontrollable factor was wind shear. The following table shows the factors considered and their possible values.

Table C-1: DOE Factors Considered

| Factors | Values |
|----------------|---|
| Pilots | -1 (Pilot 1), 0 (Pilot 2), 1 (Pilot 3) |
| Entry Airspeed | -1 (85 KIAS), 0 (95 KIAS), 1 (105 KIAS) |
| Maneuver Type | -1 (Anti-hairpin), 1 (Hairpin) |
| Wind Shear | Variable (-0.009/sec to 0.040/sec) |

The following factors and interactions were considered for the model: wind shear, wind shear squared, entry speed, entry speed squared, wind shear \times entry speed, wind shear \times entry speed squared, wind shear squared \times entry speed, and wind shear squared \times entry speed squared.

After analyzing the effects and interactions of these factors four primary effects were declared active by the DOE analysis. The magnitude of these effects is shown in Table C-2. The pilot factor was treated as a block effect, which means the only effect of the pilot was to move the model up or down, but not affect the slope. Pilots could not interact with other factors. Entry airspeed was designed as a factor, but analyzed as a continuous variable (or covariate), as some variation occurred in targeting the airspeeds. For the purposes of the DOE analysis an anti-hairpin maneuver was considered the same as a hairpin maneuver in a negative wind shear (i.e. wind speed decreasing with altitude). As maneuver type was used to apply a sign to the wind shear, it does not appear in the ANOVA table as an active effect.

Table C-2: Pitot-static Energy Model Statistics

| | Model Value | -95% Confidence | +95% Confidence | F | p-value |
|--------------------|-------------|-----------------|-----------------|--------|---------|
| Mean | -160.2 | -166.9 | -153.4 | 2213.1 | 0.0000 |
| Wind Shear | 557.3 | 336.5 | 778.1 | 25.0 | 0.0000 |
| Speed | -3.8 | -4.3 | -3.3 | 263.8 | 0.0000 |
| Speed ² | -0.09 | -0.18 | -0.003 | 4.2 | 0.0433 |
| Pilot 1,3 | 8.6 | 3.7 | 13.6 | 13.8 | 0.0000 |
| Pilot 2 | -16.1 | -22.2 | -9.94 | 13.8 | 0.0000 |

The p-value indicates the alpha error (confidence equals $1 - \alpha$ -error), which is the probability of a false positive. That is, saying that something happened, when in actuality it occurred by chance. So, in plain speak, there is a 1 in 20 chance that these Dynamic Soaring maneuvers will show the entry speed squared impacts the difference in energy height lost when it actually does not have an impact. Likewise, the F-ratio is an indication of confidence. As F-ratio increases it becomes less likely that differences in the outcome of the test are due to chance. If the factors

have no effect then the F-ratio will be near a value of one. The confidence interval indicates that 95 percent of the time the coefficients in the model should fall within the interval given.

Regarding the term power that was mentioned in the body of the report, using an α -error cut-off of 21 percent (i.e. the highest confidence term not included in the model had 21 percent alpha error associated with it) the following chart could be produced. Power, which is defined as $1 - \beta$ error, indicates how likely one is to miss a change in the response variable. Power quantifies how likely it is there is a term in the model that creates a difference of some size. The curve in Figure C-1 shows the β -error of this test. As shown below the test was capable of detecting a 10 energy height feet change 99.9 percent of the time.

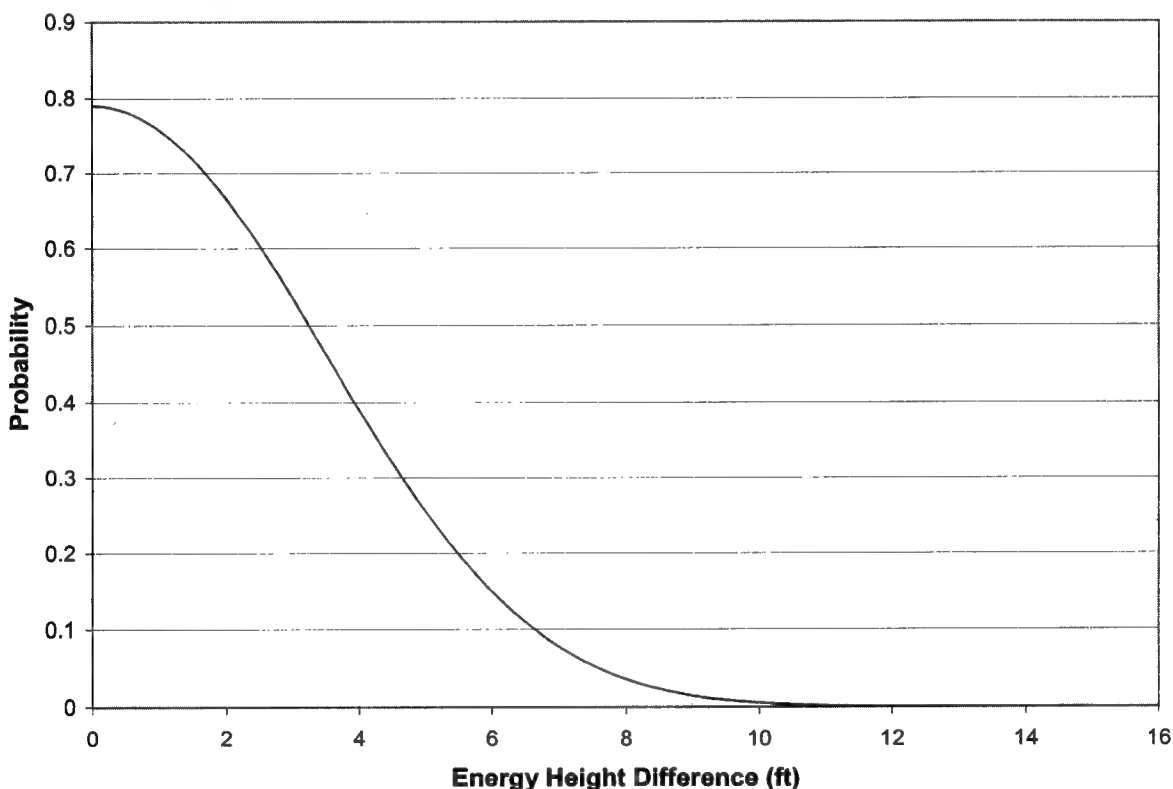


Figure C-1: Plot of the Chances of Missing a Difference in Energy Height

Appendix D: Lessons Learned

Facilities/Lakebed Operations

Operating from the lakebed and the North Base hangar was critical to efficient operations. Equally critical was the use of a fifth wheel camper that was stationed on the lakebed during operations. The camper provided protection from the winds and temperature, but more importantly it provided a power source to charge tablet PCs and radios, and operate laptop PCs and weather data gathering equipment. Without the camper, operations would have been seriously hampered resulting in reduced test efficiency. Operating from the lakebed with published glider operations NOTAMS and FCIFs allowed the team to operate nearly carefree regarding other aircraft, and provided a safety buffer since the lakebed offered a landable surface in any direction. Additionally, since the glider could be landed near the camper, crew swaps and instrumentation trouble shooting could be accomplished quickly. The North Base hangar provided a place to store the tow plane, glider, and camper. The proximity of the hangar to the lakebed also allowed the team to be fully deployed to the lakebed and ready to fly within about 15 minutes of arrival at the hangar. Finally, at least three radios should be used during glider operations. One radio needs to be located at the operating center, one in the glider, and the last one in the tow plane. Additionally, it was helpful to have a separate VHF mission frequency monitored by tower. The team was required to contact tower prior to moving onto the lakebed, and prior to each takeoff and after each landing.

Airfield Management Coordination

All the benefits of the lakebed operations can only be recognized with proper coordination with airfield management. The biggest lesson learned during SENIOR ShWOOPIN operations was that airfield management needs to be involved in the planning process from the test concept meeting onward. Depending upon the results of the test concept meeting it may also be beneficial to have airfield management present at the SRB. The test team recommends that future glider teams should address the following items in particular:

1. Every test team member should have a flight line driver's license.
2. Every test team member should get a vehicle pass for their POV to be driven on the lakebed.
3. Emphasize that you will need to operate from the lakebed for efficiency (suggest using a camper as your base of operations). Work out training details so that the test team can clear the lakebeds as safe for glider operations independent of Base Ops personnel. If this is not possible, at least make sure that airfield management is prepared to go the extra mile to declare lakebeds green for glider operations on the test team's time table.
4. Clearly identify where you intend to operate POVs around North Base and the lakebeds (including entry/exit points).

Weather Support

NASA DFRC weather support was critical to this project. During SENIOR ShWOOPIN operations the test team discovered that many of the weather data gathering systems were largely unreliable. The only reliable information came from the weather balloons. One of the more significant problems encountered with all the weather data systems was a lack of standardization

of the units of measure. To the greatest extent possible, future teams relying heavily on weather data should try to get weather data presented in a format that is recognized by pilots (i.e. magnetic heading in degrees, airspeed in knots, and pressure altitude in feet).

Instrumentation/Displays

Overall the instrumentation and display systems used in this project were satisfactory for the task. However, a few improvements would make the systems easier to use. First, the primary problem encountered with the tablet PCs was their tendency to overheat. Consider installing a small fan behind the PC to provide cooling. Related to this problem was the shutdown sequence for the tablet PC. If the tablet PC in the front cockpit needed to be replaced due to overheating, then the entire instrumentation system had to be shutdown. A shutdown/restart sequence required 10-15 min primarily because of the time required for the INS/GPS to realign. Additionally, one of the power switches (P2) was located behind the seat in the rear cockpit, which meant that the power sequence required the FTE to unstrap. Explore the possibility of a tablet PC to GS-111m interface that does not require a shutdown/restart sequence in order to swap the front cockpit tablet PC. Likewise, move the P2 power switch to the instrumentation power panel in the front cockpit.

Prior to flying there was some concern over the ability of the tablet PC's hard drive to survive the required g loading during the Dynamic Soaring maneuver. However, the tablet PC's hard drive performed very well, and the only noted problem was the tendency to overheat that was previously mentioned. Additionally, the anti-glare screen on the tablet PC was a notable improvement over the standard screen on clear days. The tablet PC was used as the sole source to record data instead of the GS-111m because it was much easier to transfer files from the PC using the Windows environment instead of using the point-to-point protocol terminal on the laptop to interface with the GS-111m. The GS-111m recorded data files as a backup, but the tablet PC proved to be very reliable.

The total energy gauge (an altimeter plumbed to the total energy variometer probe) worked well as an independent source of energy height information. The displayed total energy height on the gauge matched the Pitot-static energy height on the tablet PC within 10-20 feet throughout the flights. This provided the quickest feedback in-flight regarding the energy state of the glider and how much energy had been lost during a maneuver. The total energy gauge became the primary source for hand held data taken during the sortie along with the maneuver start time to match hand held data with the recorded data files.

Simulator

Generally, the simulator was an effective tool for practicing the DS FTT, assessing the original aerodynamic model used in theory formulation, and refining crew coordination procedures. There were some inconsistencies between the handling qualities of the simulator and the actual glider. Specifically, the stick forces (all axes) observed in the simulator were greater than those experienced in the glider. Therefore, adjustments to the simulator stick force bellows were accomplished in order to better duplicate actual control stick forces. In addition, lateral-directional control was difficult to maintain due to excessive adverse yaw effects from aileron deflections. This was remedied by increasing the $C_{n\beta}$ and reducing the $C_{l\delta a}$ stability derivatives in the simulator. However, rudder could not be used in the simulator without exciting a large

amplitude Dutch Roll mode that was uncharacteristic of the glider. For this reason maneuvers were executed using only the center stick. Future glider projects should focus on improving the lateral directional stability derivatives used in the simulation model. Nonetheless, even with these limitations, the simulator flew well enough to practice DS FTTs. This was beneficial for refining maneuver quality and delegating crew responsibilities.

This page intentionally left blank.

Appendix E: Total Energy Probe Theory

(Adapted from notes by Mr. Joe Wurts, Lockheed-Martin Engineer and Dynamic Soaring expert.)

The total energy for an aircraft is defined as the sum of the kinetic energy, and the potential energy due to altitude and gravity.

$$E = \frac{1}{2}mV^2 + mgh \quad \text{Eq. 1}$$

Where m is the mass, V is velocity, g is acceleration due to gravity, and h is the current altitude.

Dividing by mg allows us to define specific energy height (units in feet):

$$E_s = \frac{V^2}{2g} + h \quad \text{Eq. 2}$$

The first term in this equation is the kinetic energy expressed in units of altitude, and is the amount of energy gained when something drops from the specific total energy altitude to the current altitude. The second term is simply the current altitude.

The change in static atmospheric pressure between the total energy height and the current height can be defined as

$$\Delta p = -\rho g \Delta h \quad \text{Eq. 3}$$

assuming that the change in air density between these two altitudes is small compared to the total density (i.e., incompressible theory, which holds up quite well for sailplanes). Here ρ is air density and Δh is the difference in altitude between the total energy height and the current altitude.

Then from the second equation above, and assuming a constant total energy, it can be shown that:

$$\Delta h = \frac{V^2}{2g} \quad \text{Eq. 4}$$

Substituting Δh from Eq. 4 into Eq. 3 provides the definition of the change in static pressure between the total energy height and the current height as:

$$\Delta p = -\frac{1}{2}\rho V^2 \quad \text{Eq. 5}$$

From Bernoulli's equation we know the dynamic pressure due to the flight velocity is:

$$\bar{q} = \frac{1}{2}\rho V^2 \quad \text{Eq. 6}$$

The \bar{q} term is the difference between the total pressure and the static pressure measured by a Pitot-static tube, assuming the c_p on the total pressure is +1. By comparing Eq. 5 and Eq. 6, the conclusion can be drawn that the change in static pressure between the total energy height and the current height is the negative of the dynamic pressure. To obtain the total energy height in terms of pressure, all one needs to do is find a measurement of negative dynamic pressure, i.e. find a source for a c_p of -1, and measure the pressure from this source.

The sailplane community long ago worked this out, and found that a suitable source of negative dynamic pressure can be obtained on the back portion of a cylinder oriented perpendicular to the airflow. An altimeter that is connected to the same line as a typical total energy variometer that is mounted in a sailplane will show the total energy height as its displayed altitude. Neglecting drag, the altitude shown on the altimeter would be the altitude that one could achieve if one converted the flight speed back into altitude.

Appendix F: Flight Test Results

The table below shows the data points collected during the course of the test window. The data shaded in gray was not used in the data analysis because the wind data was questionable.

NOSHEAR

SIGNIFICANT SHEAR

1999, 2000, 2001, 2002, 2003, 2004, 2005, 2006, 2007, 2008, 2009, 2010, 2011, 2012, 2013, 2014, 2015, 2016, 2017, 2018, 2019, 2020, 2021, 2022, 2023, 2024, 2025, 2026, 2027, 2028, 2029, 2030, 2031, 2032, 2033, 2034, 2035, 2036, 2037, 2038, 2039, 2040, 2041, 2042, 2043, 2044, 2045, 2046, 2047, 2048, 2049, 2050, 2051, 2052, 2053, 2054, 2055, 2056, 2057, 2058, 2059, 2060, 2061, 2062, 2063, 2064, 2065, 2066, 2067, 2068, 2069, 2070, 2071, 2072, 2073, 2074, 2075, 2076, 2077, 2078, 2079, 2080, 2081, 2082, 2083, 2084, 2085, 2086, 2087, 2088, 2089, 2090, 2091, 2092, 2093, 2094, 2095, 2096, 2097, 2098, 2099, 2100, 2101, 2102, 2103, 2104, 2105, 2106, 2107, 2108, 2109, 2110, 2111, 2112, 2113, 2114, 2115, 2116, 2117, 2118, 2119, 2120, 2121, 2122, 2123, 2124, 2125, 2126, 2127, 2128, 2129, 2130, 2131, 2132, 2133, 2134, 2135, 2136, 2137, 2138, 2139, 2140, 2141, 2142, 2143, 2144, 2145, 2146, 2147, 2148, 2149, 2150, 2151, 2152, 2153, 2154, 2155, 2156, 2157, 2158, 2159, 2160, 2161, 2162, 2163, 2164, 2165, 2166, 2167, 2168, 2169, 2170, 2171, 2172, 2173, 2174, 2175, 2176, 2177, 2178, 2179, 2180, 2181, 2182, 2183, 2184, 2185, 2186, 2187, 2188, 2189, 2190, 2191, 2192, 2193, 2194, 2195, 2196, 2197, 2198, 2199, 2200, 2201, 2202, 2203, 2204, 2205, 2206, 2207, 2208, 2209, 2210, 2211, 2212, 2213, 2214, 2215, 2216, 2217, 2218, 2219, 2220, 2221, 2222, 2223, 2224, 2225, 2226, 2227, 2228, 2229, 2230, 2231, 2232, 2233, 2234, 2235, 2236, 2237, 2238, 2239, 2240, 2241, 2242, 2243, 2244, 2245, 2246, 2247, 2248, 2249, 2250, 2251, 2252, 2253, 2254, 2255, 2256, 2257, 2258, 2259, 2260, 2261, 2262, 2263, 2264, 2265, 2266, 2267, 2268, 2269, 2270, 2271, 2272, 2273, 2274, 2275, 2276, 2277, 2278, 2279, 2280, 2281, 2282, 2283, 2284, 2285, 2286, 2287, 2288, 2289, 2290, 2291, 2292, 2293, 2294, 2295, 2296, 2297, 2298, 2299, 2300, 2301, 2302, 2303, 2304, 2305, 2306, 2307, 2308, 2309, 2310, 2311, 2312, 2313, 2314, 2315, 2316, 2317, 2318, 2319, 2320, 2321, 2322, 2323, 2324, 2325, 2326, 2327, 2328, 2329, 2330, 2331, 2332, 2333, 2334, 2335, 2336, 2337, 2338, 2339, 2340, 2341, 2342, 2343, 2344, 2345, 2346, 2347, 2348, 2349, 2350, 2351, 2352, 2353, 2354, 2355, 2356, 2357, 2358, 2359, 2360, 2361, 2362, 2363, 2364, 2365, 2366, 2367, 2368, 2369, 2370, 2371, 2372, 2373, 2374, 2375, 2376, 2377, 2378, 2379, 2380, 2381, 2382, 2383, 2384, 2385, 2386, 2387, 2388, 2389, 2390, 2391, 2392, 2393, 2394, 2395, 2396, 2397, 2398, 2399, 2400, 2401, 2402, 2403, 2404, 2405, 2406, 2407, 2408, 2409, 2410, 2411, 2412, 2413, 2414, 2415, 2416, 2417, 2418, 2419, 2420, 2421, 2422, 2423, 2424, 2425, 2426, 2427, 2428, 2429, 2430, 2431, 2432, 2433, 2434, 2435, 2436, 2437, 2438, 2439, 2440, 2441, 2442, 2443, 2444, 2445, 2446, 2447, 2448, 2449, 2450, 2451, 2452, 2453, 2454, 2455, 2456, 2457, 2458, 2459, 2460, 2461, 2462, 2463, 2464, 2465, 2466, 2467, 2468, 2469, 2470, 2471, 2472, 2473, 2474, 2475, 2476, 2477, 2478, 2479, 2480, 2481, 2482, 2483, 2484, 2485, 2486, 2487, 2488, 2489, 2490, 2491, 2492, 2493, 2494, 2495, 2496, 2497, 2498, 2499, 2500, 2501, 2502, 2503, 2504, 2505, 2506, 2507, 2508, 2509, 2510, 2511, 2512, 2513, 2514, 2515, 2516, 2517, 2518, 2519, 2520, 2521, 2522, 2523, 2524, 2525, 2526, 2527, 2528, 2529, 2530, 2531, 2532, 2533, 2534, 2535, 2536, 2537, 2538, 2539, 2540, 2541, 2542, 2543, 2544, 2545, 2546, 2547, 2548, 2549, 2550, 2551, 2552, 2553, 2554, 2555, 2556, 2557, 2558, 2559, 2560, 2561, 2562, 2563, 2564, 2565, 2566, 2567, 2568, 2569, 2570, 2571, 2572, 2573, 2574, 2575, 2576, 2577, 2578, 2579, 2580, 2581, 2582, 2583, 2584, 2585, 2586, 2587, 2588, 2589, 2590, 2591, 2592, 2593, 2594, 2595, 2596, 2597, 2598, 2599, 2600, 2601, 2602, 2603, 2604, 2605, 2606, 2607, 2608, 2609, 2610, 2611, 2612, 2613, 2614, 2615, 2616, 2617, 2618, 2619, 2620, 2621, 2622, 2623, 2624, 2625, 2626, 2627, 2628, 2629, 2630, 2631, 2632, 2633, 2634, 2635, 2636, 2637, 2638, 2639, 2640, 2641, 2642, 2643, 2644, 2645, 2646, 2647, 2648, 2649, 2650, 2651, 2652, 2653, 2654, 2655, 2656, 2657, 2658, 2659, 2660, 2661, 2662, 2663, 2664, 2665, 2666, 2667, 2668, 2669, 2670, 2671, 2672, 2673, 2674, 2675, 2676, 2677, 2678, 2679, 2680, 26

Table F-2: 90-100 KIAS Entry Speed Data Points

| Date | Time (L) | Hairpin or Anti-Hairpin | Aircrew | Entry Airspeed (KIAS) | Entry Altitude Baro Interfial (ft) | Wind Shear (1/s) | Wind Direction | Mnvr Run- in Heading | Pilot- static ΔEs | Pilot- static Max Es | Geometric ΔEs | Geometric Max Es | Exit Airspeed (KIAS) | Exit Altitude (ft) | NO SHEAR |
|-----------|----------|----------------------------|-------------|-----------------------------|---|------------------------|-------------------|----------------------------|-------------------------|----------------------------|------------------|---------------------|----------------------------|--------------------------|-------------------|
| 10-Apr-06 | 8:23:41 | Anti-Hairpin | Sol/T2 | 94 | 3166 | 0.007 | 235 | 028 | -155 | 0 | -245 | 0 | 79 | 4200 | |
| 10-Apr-06 | 8:28:21 | Anti-Hairpin | Sol/T2 | 94 | 4020 | 0.002 | 225 | 209 | -205 | 0 | -161 | 0 | 79 | 4040 | |
| 10-Apr-06 | 9:41:44 | Hairpin | Sol/T2 | 94 | 3166 | 0.007 | 235 | 213 | -128 | 0 | -327 | 0 | 79 | 4200 | |
| 10-Apr-06 | 12:22:21 | Anti-Hairpin | Laz/Eck | 94 | 4220 | -0.007 | 235 | 330 | -160 | 12 | -170 | 22 | 79 | 4200 | |
| 10-Apr-06 | 12:21:12 | Anti-Hairpin | Laz/Eck | 96 | 4800 | -0.007 | 235 | 160 | -147 | 23 | -150 | 17 | 79 | 4840 | |
| 21-Apr-06 | 10:36:37 | Anti-Hairpin | Laz/T2 | 94 | 3125 | -0.004 | 240 | 330 | -175 | 5 | -182 | 0 | 75 | 3120 | |
| 28-Apr-06 | 9:13:34 | Anti-Hairpin | Riddler/Eck | 94 | 4514 | 0.004 | 001 | 082 | -139 | 0 | -134 | 28 | 80 | 4513 | |
| 3-May-06 | 9:23:05 | Anti-Hairpin | Sol/T2 | 95 | 4721 | 0.005 | 305 | 230 | -130 | 9 | -133 | 26 | 78 | 4749 | |
| 24-Apr-06 | 8:06:35 | Anti-Hairpin | Sol/T2 | 94 | 3550 | 0.010 | 340 | 228 | -163 | 3 | -153 | 0 | 71 | 3580 | |
| 14-Apr-06 | 8:58:49 | Anti-Hairpin | Sol/Erb | 94 | 3743 | 0.010 | 235 | 326 | -142 | 0 | -167 | 0 | 76 | 3767 | |
| 21-Apr-06 | 12:07:16 | Hairpin | Laz/Eck | 95 | 4600 | -0.007 | 235 | 152 | -149 | 17 | -191 | 0 | 74 | 4650 | |
| 10-Apr-06 | 12:08:21 | Hairpin | Laz/Eck | 95 | 3800 | -0.007 | 235 | 323 | -178 | 0 | -165 | 10 | 74 | 3800 | |
| 21-Apr-06 | 10:15:57 | Hairpin | Laz/T2 | 92 | 3030 | 0.001 | 240 | 328 | -150 | 18 | -173 | 0 | 71 | 3040 | |
| 28-Apr-06 | 8:58:32 | Hairpin | Riddler/Eck | 94 | 4523 | 0.004 | 001 | 085 | -139 | 8 | -146 | 3 | 77 | 4543 | |
| 24-Apr-06 | 7:40:10 | Hairpin | Sol/T2 | 93 | 3506 | 0.010 | 340 | 233 | -114 | 0 | -143 | 0 | 77 | 3523 | |
| 17-Apr-06 | 7:57:17 | Hairpin | Sol/T2 | 93 | 4082 | 0.005 | 250 | 180 | -233 | 0 | -287 | 0 | 81 | 4091 | |
| Date | Time (L) | Hairpin or Anti-Hairpin | Aircrew | Entry Airspeed (KIAS) | Entry Altitude Baro Interfial (ft) | Wind Shear (1/s) | Wind Direction | Mnvr Run- in Heading | Pilot- static ΔEs | Pilot- static Max Es | Geometric ΔEs | Geometric Max Es | Exit Airspeed (KIAS) | Exit Altitude (ft) | SIGNIFICANT SHEAR |
| 28-Apr-06 | 9:16:12 | Anti-Hairpin | Riddler/Eck | 94 | 3160 | 0.011 | 330 | 273 | -175 | 6 | -185 | 0 | 72 | 3157 | |
| 3-May-06 | 7:24:17 | Anti-Hairpin | Laz/Eck | 95 | 3640 | 0.011 | 270 | 320 | -217 | 0 | -206 | 0 | 71 | 3627 | |
| 14-Apr-06 | 9:21:42 | Anti-Hairpin | Sol/Erb | 94 | 3858 | 0.014 | 235 | 318 | -127 | 0 | -133 | 18 | 77 | 3878 | |
| 28-Apr-06 | 7:45:10 | Anti-Hairpin | Riddler/T2 | 94 | 3446 | 0.019 | 000 | 100 | -125 | 0 | -174 | 0 | 74 | 3484 | |
| 14-Apr-06 | 9:00:57 | Anti-Hairpin | Sol/Erb | 93 | 2911 | 0.016 | 235 | 148 | -151 | 9 | -185 | 17 | 71 | 2944 | |
| 28-Apr-06 | 9:14:23 | Anti-Hairpin | Riddler/Eck | 95 | 4015 | 0.028 | 003 | 091 | -196 | 0 | -235 | 0 | 74 | 4005 | |
| 28-Apr-06 | 9:15:23 | Anti-Hairpin | Riddler/Eck | 95 | 3507 | 0.030 | 360 | 271 | -162 | 7 | -167 | 0 | 75 | 3520 | |
| 28-Apr-06 | 7:44:11 | Anti-Hairpin | Riddler/T2 | 95 | 4049 | 0.030 | 003 | 284 | -175 | 8 | -224 | 6 | 78 | 4042 | |
| 17-Apr-06 | 7:58:14 | Anti-Hairpin | Sol/T2 | 92 | 3262 | 0.039 | 302 | 335 | -217 | 0 | -185 | 118 | 81 | 3289 | |
| 17-Apr-06 | 7:59:07 | Hairpin | Sol/T2 | 91 | 2594 | 0.021 | 287 | 332 | -154 | 56 | -78 | 230 | 80 | 2660 | |
| 17-Apr-06 | 9:59:14 | Hairpin | Laz/Erb | 95 | 2700 | 0.027 | 234 | 153 | -172 | 1 | -182 | 2 | 74 | 2720 | |
| 17-Apr-06 | 9:57:14 | Hairpin | Laz/Erb | 95 | 2690 | 0.027 | 234 | 140 | -178 | 0 | -187 | 30 | 75 | 2700 | |
| 28-Apr-06 | 9:01:12 | Hairpin | Riddler/Eck | 94 | 3262 | 0.011 | 330 | 274 | -151 | 0 | -142 | 0 | 79 | 3260 | |
| 3-May-06 | 9:00:37 | Hairpin | Sol/T2 | 95 | 4781 | 0.012 | 305 | 050 | -143 | 1 | -147 | 0 | 78 | 4809 | |
| 28-Apr-06 | 7:21:55 | Hairpin | Laz/Eck | 95 | 5026 | 0.013 | 320 | 318 | -166 | 0 | -162 | 4 | 72 | 5070 | |
| 14-Apr-06 | 7:28:24 | Hairpin | Riddler/T2 | 94 | 3519 | 0.014 | 340 | 096 | -118 | 6 | -129 | 0 | 79 | 3546 | |
| 14-Apr-06 | 8:50:27 | Hairpin | Sol/Erb | 93 | 2819 | 0.021 | 235 | 150 | -167 | 0 | -152 | 53 | 71 | 2836 | |
| 14-Apr-06 | 9:24:34 | Hairpin | Sol/Erb | 94 | 2750 | 0.024 | 235 | 160 | -192 | 0 | -186 | -21 | 69 | 2769 | |
| 28-Apr-06 | 8:59:17 | Hairpin | Riddler/Eck | 94 | 4045 | 0.028 | 003 | 094 | -124 | 10 | -121 | 25 | 80 | 4065 | |
| 28-Apr-06 | 9:00:21 | Hairpin | Riddler/Eck | 96 | 3608 | 0.030 | 360 | 272 | -122 | 0 | -135 | 0 | 82 | 3620 | |
| 28-Apr-06 | 7:27:07 | Hairpin | Riddler/T2 | 97 | 4080 | 0.040 | 010 | 281 | -150 | 0 | -160 | 0 | 78 | 4099 | |

Table F-3: 100-110 KIAS Entry Speed Data Points

| Date | Time (L) | Hairstrip or Anti-Hairstrip | Aircrew | Entry Airspeed (KIAS) | Entry Altitude Baro Interstitial (ft) | Wind Shear (ft/s) | Wind Direction | Minvr Run-In Heading | Pilot-static ΔEs | Pilot-static Max Es | Geometric ΔEs | Geometric Max Es | Exit Airspeed (KIAS) | Exit Altitude (ft) | NO SHEAR |
|-----------|----------|-----------------------------|---------------|-----------------------|---------------------------------------|-------------------|----------------|----------------------|------------------|---------------------|---------------|------------------|----------------------|--------------------|----------|
| 10-Apr-06 | 9:10:22 | Hairstrip | Sol/T2 | 101 | 4007 | -0.002 | 225 | 200 | -208 | 0 | -175 | 0 | 81 | 3991 | |
| 21-Apr-06 | 10:14:33 | Anti-Hairstrip | Laz/T2 | 101 | 3760 | -0.001 | 250 | 140 | -220 | 0 | -255 | 0 | 80 | 3770 | |
| 24-Apr-06 | 8:53:06 | Anti-Hairstrip | Ridder/Lester | 104 | 3080 | 0.001 | 188 | 228 | -180 | 0 | -103 | 0 | 85 | 3096 | |
| 3-May-06 | 8:05:27 | Anti-Hairstrip | Laz/Eck | 103 | 4715 | 0.005 | 315 | 080 | -222 | 0 | -239 | 0 | 80 | 4720 | |
| 24-Apr-06 | 10:33:14 | Anti-Hairstrip | Sol/Eck | 104 | 3956 | 0.006 | 240 | 320 | -205 | 0 | -237 | 0 | 86 | 3950 | |
| 19-Apr-06 | 7:49:21 | Anti-Hairstrip | Laz/Eck | 103 | 3020 | 0.008 | 60 | 140 | -227 | 0 | -247 | 0 | 75 | 3060 | |
| 3-May-06 | 9:24:26 | Anti-Hairstrip | Sol/T2 | 104 | 3952 | 0.009 | 270 | 053 | -181 | 7 | -207 | 0 | 90 | 3918 | |
| 26-Apr-06 | 7:48:39 | Anti-Hairstrip | Ridder/Eck | 104 | 6060 | 0.010 | 145 | 360 | -211 | 0 | -212 | 0 | 86 | 6043 | |
| 3-May-06 | 8:46:01 | Anti-Hairstrip | Sol/T2 | 104 | 4775 | 0.010 | 315 | 053 | -210 | 0 | -218 | 0 | 86 | 4767 | |
| 21-Apr-06 | 10:35:29 | Hairstrip | Laz/T2 | 108 | 3900 | -0.001 | 250 | 150 | -230 | 0 | -208 | 0 | 80 | 3930 | |
| 24-Apr-06 | 8:40:33 | Hairstrip | Ridder/Lester | 103 | 3065 | 0.001 | 188 | 236 | -177 | 0 | -169 | 0 | 82 | 3105 | |
| 24-Apr-06 | 9:33:36 | Hairstrip | Sol/Eck | 103 | 4219 | 0.003 | 320 | 051 | -181 | 21 | -234 | 0 | 89 | 4188 | |
| 3-May-06 | 7:51:15 | Hairstrip | Laz/Eck | 105 | 4803 | 0.005 | 315 | 047 | -242 | 0 | -257 | 0 | 80 | 4823 | |
| 19-Apr-06 | 7:07:33 | Hairstrip | Laz/G-man | 103 | 3140 | 0.008 | 60 | 145 | -215 | 4 | -214 | 0 | 78 | 3170 | |
| 3-May-06 | 8:27:20 | Hairstrip | Sol/T2 | 104 | 4800 | 0.008 | 325 | 227 | -214 | 0 | -194 | 0 | 80 | 4827 | |
| 24-Apr-06 | 10:20:28 | Hairstrip | Sol/Eck | 105 | 3811 | 0.009 | 240 | 322 | -183 | 12 | -211 | 0 | 88 | 3790 | |
| 3-May-06 | 7:23:03 | Hairstrip | Laz/Eck | 103 | 4278 | 0.010 | 300 | 140 | -220 | 0 | -257 | 0 | 77 | 4305 | |
| 21-Apr-06 | 10:12:47 | Hairstrip | Laz/T2 | 104 | 4010 | 0.007 | 270 | 095 | -200 | 0 | -231 | 0 | 82 | 4230 | |
| 28-Apr-06 | 8:05:38 | Hairstrip | Ridder/Eck | 103 | 3777 | -0.013 | 225 | 321 | -377 | 0 | -170 | 0 | 83 | 3117 | |
| 26-Apr-06 | 8:37:56 | Hairstrip | Ridder/Eck | 105 | 3824 | 0.013 | 224 | 318 | -105 | 0 | -153 | 0 | 83 | 3821 | |
| 28-Apr-06 | 7:26:17 | Hairstrip | Ridder/T2 | 105 | 4542 | 0.036 | 010 | 269 | -198 | 0 | -181 | 8 | 85 | 4561 | |

Appendix G: Data Anomalies

Several data points from two different days were discarded from both analysis methods because the wind data from these two days were either suspect or not collected in a timely manner. For instance, most of the data points flown by pilot 1 at 95 KIAS occurred on 10 April 2006, which happened to coincide with minimal weather data collection. Specifically, only one weather balloon was launched, and furthermore, the weather data was collected about 2 hours after the data flights were completed. Not only did this prevent the team from targeting shear layers during the flights, but it called into question the accuracy of the wind data attributed to these test points. This emphasizes the need for timely weather data collected at short time intervals.

Additional data points were removed from the data analysis for flights on 17 April 2006. These data points were removed because the wind data gathered during the test points were questionable. The data were not gathered using the NASA weather balloons due to a system malfunction. Instead data collected from an Edwards AFB balloon launched prior to the flights was used as the weather reference. However, the wind speeds shown by the balloon did not match the winds experienced by the test team or the wind calls from the control tower. The disparity was likely due to a weather system that was moving through the local area during the testing, which caused localized wind shears. All three of the test points that occurred during a single sortie on this day showed up as significant outliers. Of particular note is that, a hairpin maneuver flown during this sortie resulted in a loss of only 15 feet of energy height. During this maneuver the aircrew clearly experienced the existence of a strong shear layer (much stronger than any shear layers felt throughout the rest of the program). (The aircrew generally noted shear layer entry throughout the test program by the existence of turbulence, which could be felt in the seat of the pants.) However, the wind data from the USAF balloon did not show this shear layer.

This sortie provided a good indication that not only does the phenomenon of Dynamic Soaring exist, but the effect of the phenomenon increases with increasing wind shear strength. Additionally, the data from 17 April indicate the need for precise and accurate wind data collection capabilities.

These data from 10 and 17 April 2006 are shaded in gray in the tables in Appendix F: Flight Test Results.

This page intentionally left blank.

Appendix H: Energy Height Plot Description

The following figures were used to illustrate common trends noted in the energy height losses during data analysis.

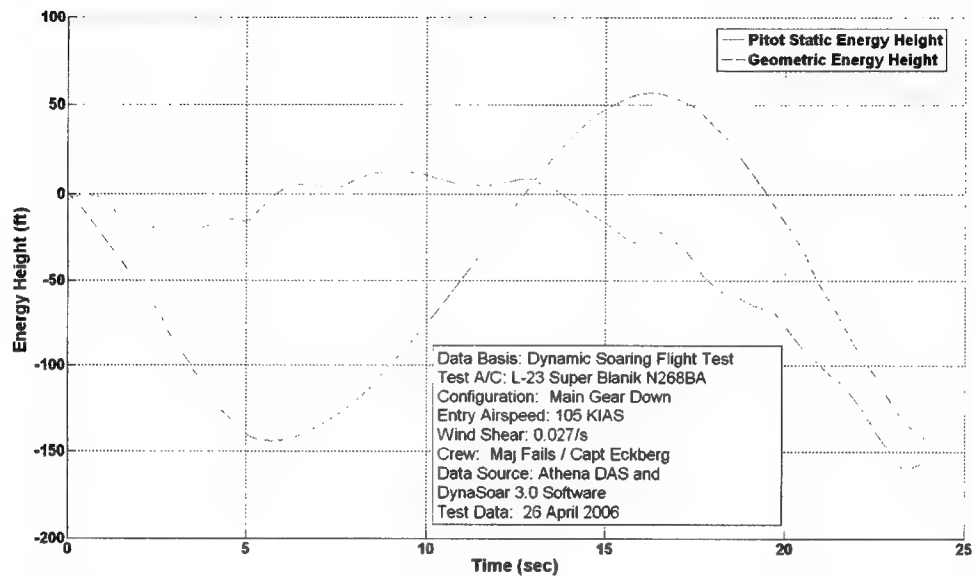


Figure H-1: Hairpin Maneuver Pitot-static and Geometric Energy Loss in a Horizontal Wind Shear

Figure H-1 illustrates the sailplane energy state experienced during a typical hairpin maneuver in wind shear. Generally, the Pitot-static energy height was characterized by a shallow decrease or increase in energy height until the aircraft reached the apex of the maneuver. The Pitot-static energy height then decreased sharply as the aircraft accelerated in the descent with the tailwind back to the entry altitude and heading. The geometric energy height was typically characterized by a sharp decrease in energy height while the sailplane was turning to climb into the headwind. Geometric energy height then sharply increased while the sailplane climbed into the wind shear. The geometric energy height decreased at roughly the same rate as the Pitot-static energy height once established in the descent back to entry altitude and heading.

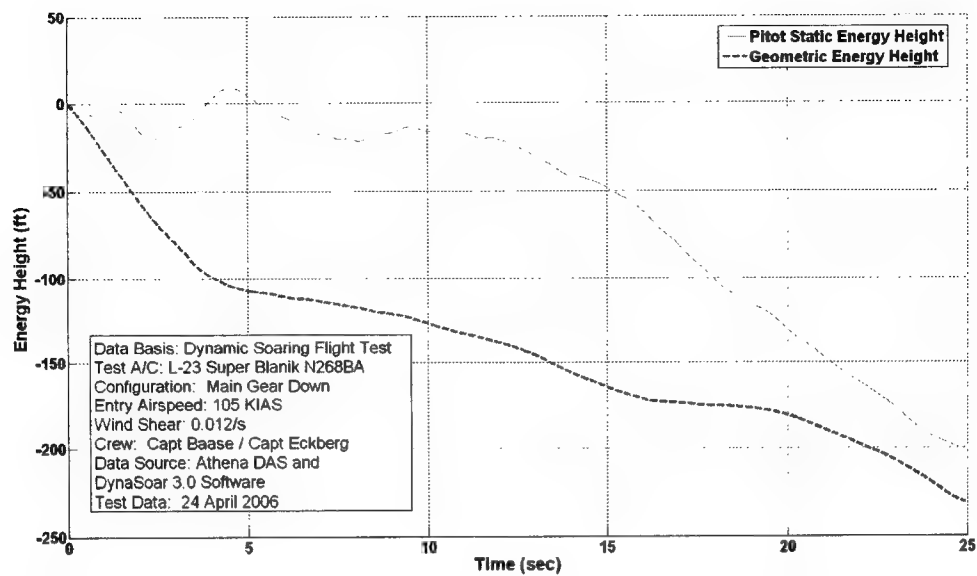


Figure H-2: Anti-Hairpin Maneuver Pitot-static and Geometric Energy Loss in a Horizontal Wind Shear

Figure H-2 illustrates the sailplane energy state experienced during a typical anti hairpin maneuver in wind shear. Generally, the Pitot-static and geometric energy heights decreased steadily throughout the maneuver.

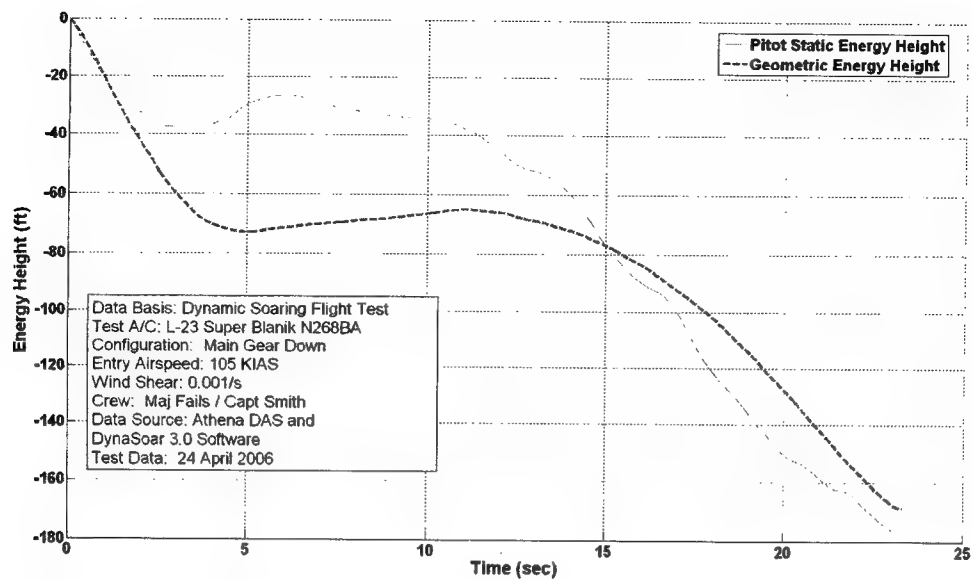


Figure H-3: No Shear Dynamic Soaring Maneuver Pitot-static and Geometric Energy Loss

Figure H-3 illustrates the sailplane energy state experienced during a typical DS FTT maneuver in wind shear. Generally, the Pitot-static and geometric energy heights decreased steadily throughout the maneuver, but the final energy states were greater than those experienced during anti-hairpin maneuvers in wind shear.

As illustrated in Table 2 and Figure H-1 through Figure H-3 performing the hairpin in wind shear resulted in a net energy loss less than that experienced when flying the hairpin in no wind shear. Thus, a full size sailplane did extract energy from a horizontal wind shear.

Appendix I: Plots of Energy Height Lost Using the Averaging Method

The following plots show the energy height lost during all three maneuvers (hairpin, anti-hairpin, and DS FTT with no shear). The maneuvers are blocked by pilot, and presented as a grand average at each entry airspeed condition. The energy lost plots are presented for both Pitot-static and geometric derived energy height.

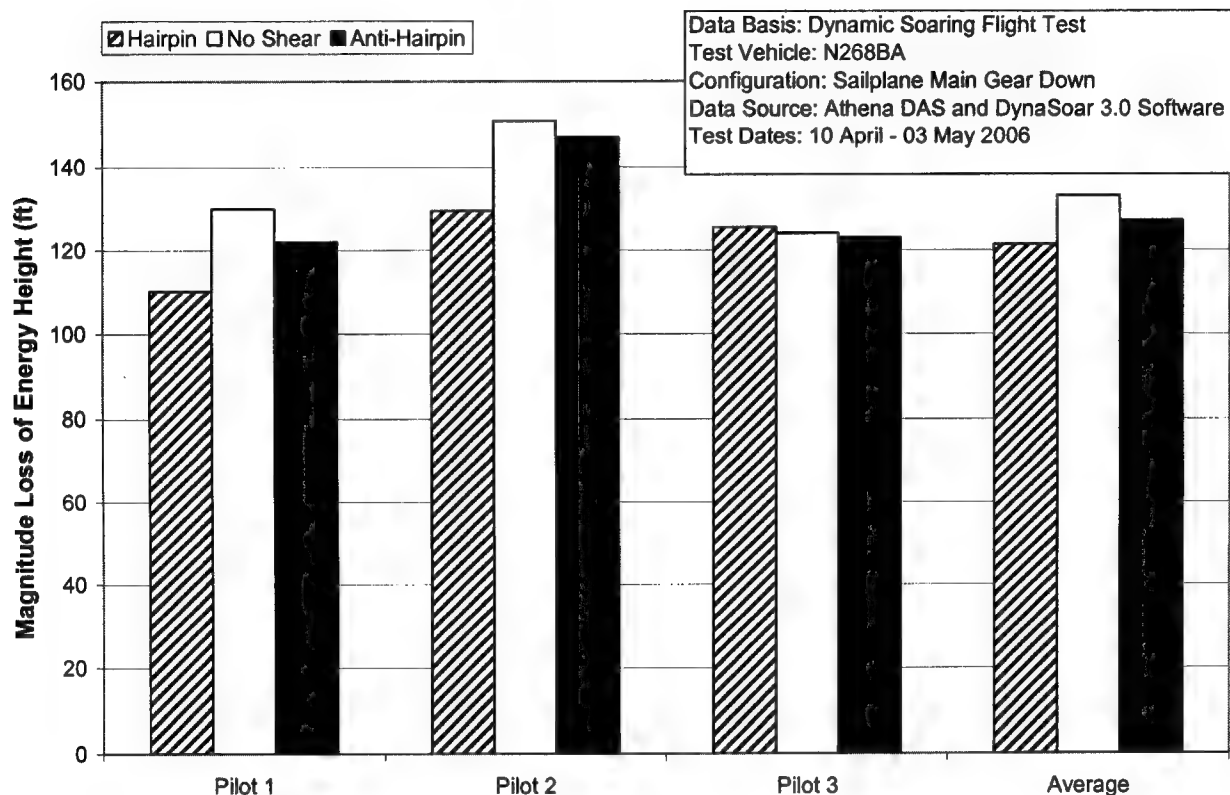


Figure I-1: Pitot-static Energy Height Loss for 85 KIAS Maneuvers

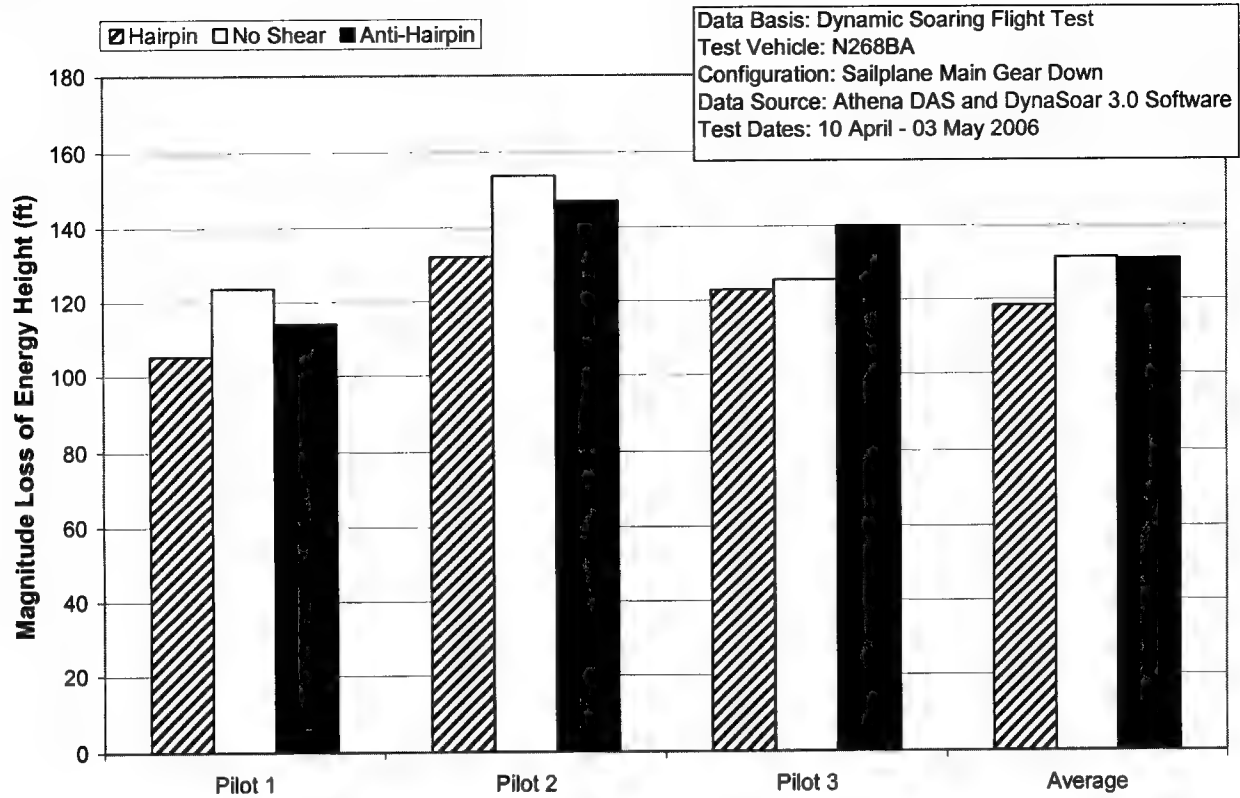


Figure I-2: Geometric Energy Height Loss for 85 KIAS Maneuvers

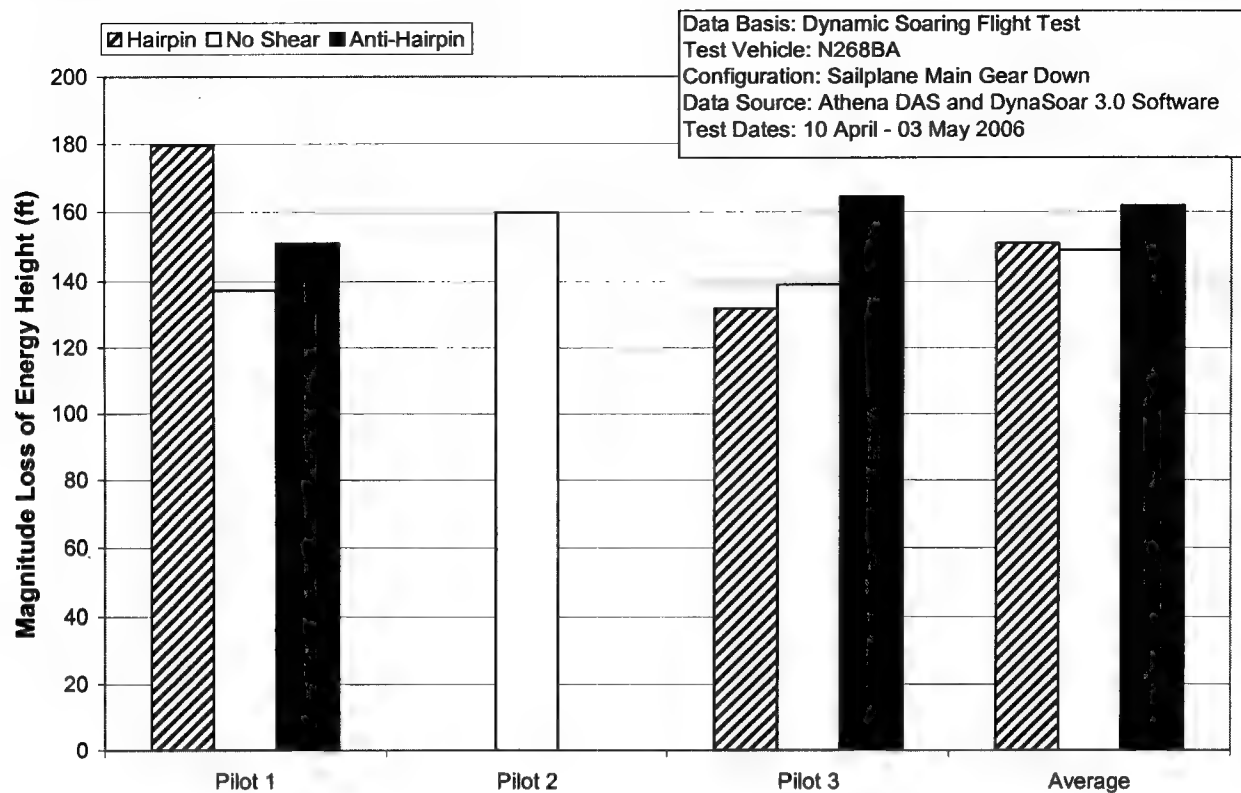


Figure I-3: Pitot-static Energy Height Loss for 95 KIAS Maneuvers

Note: Pilot 2 did not fly anti-hairpin or hairpin maneuvers in a shear at 95 KIAS.

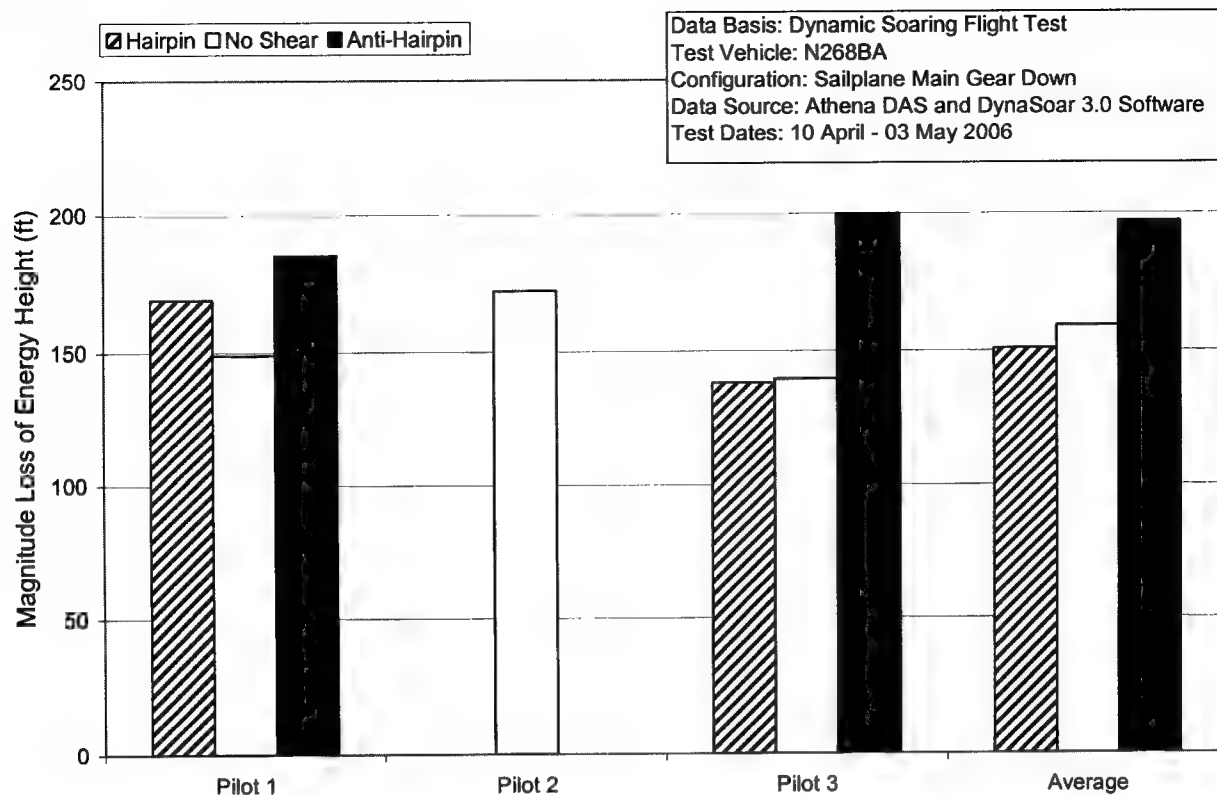


Figure I-4: Geometric Energy Height Loss for 95 KIAS Maneuvers

Note: Pilot 2 did not fly anti-hairpin or hairpin maneuvers in a shear at 95 KIAS.

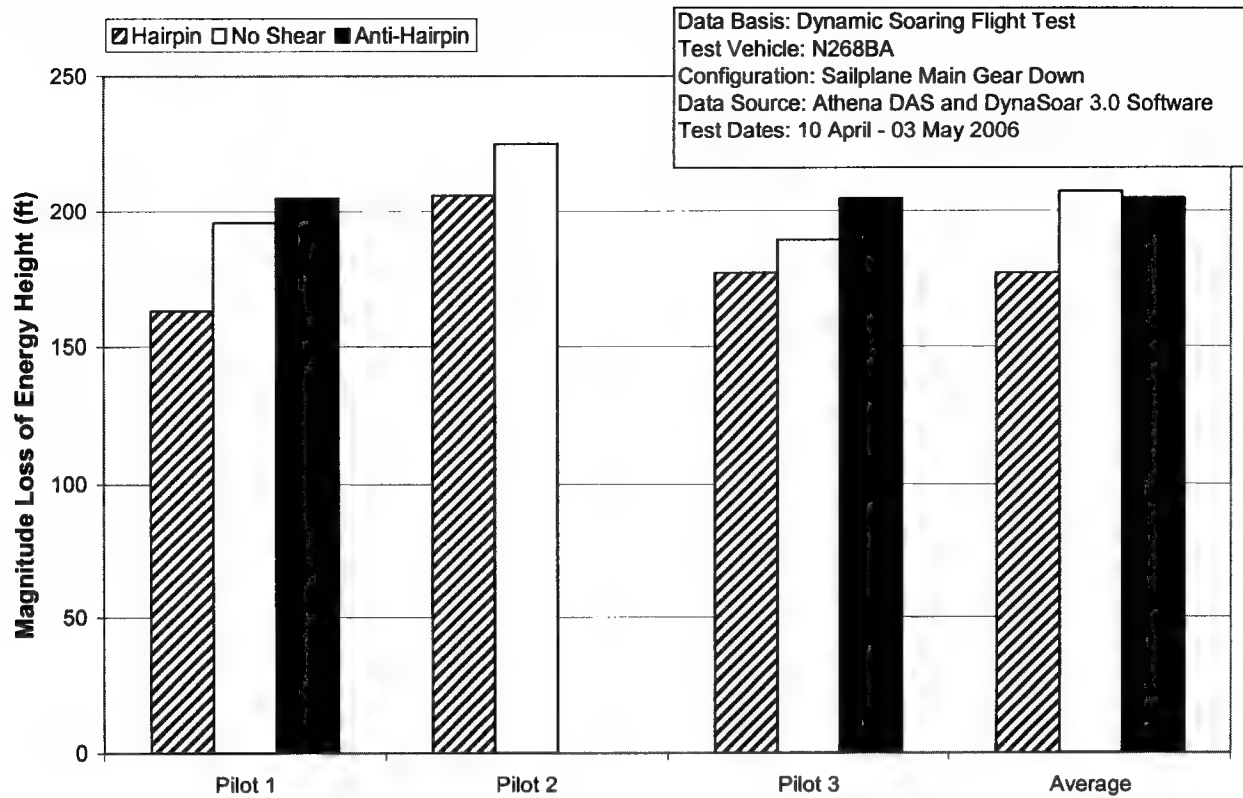


Figure I-5: Pitot-static Energy Height Loss for 105 KIAS Maneuvers

Note: Pilot 2 did not fly anti-hairpin maneuvers in a shear at 105 KIAS.

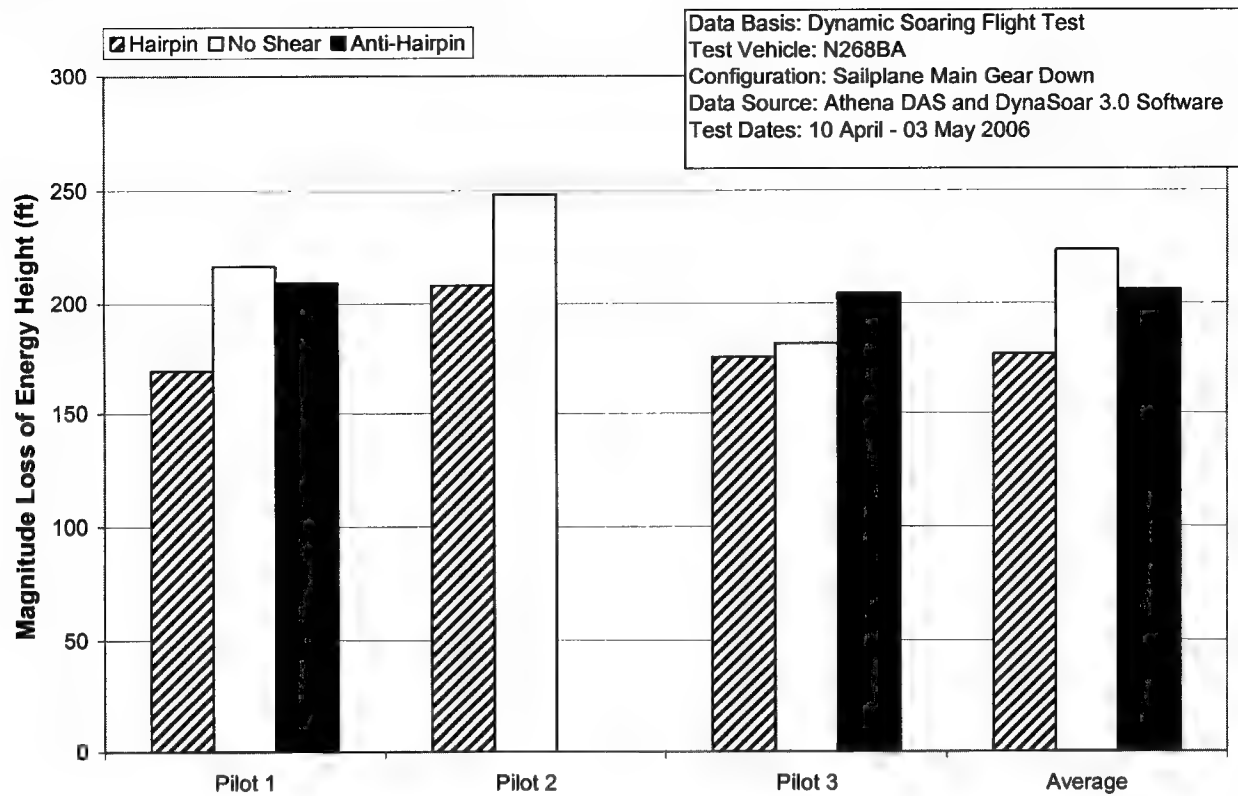
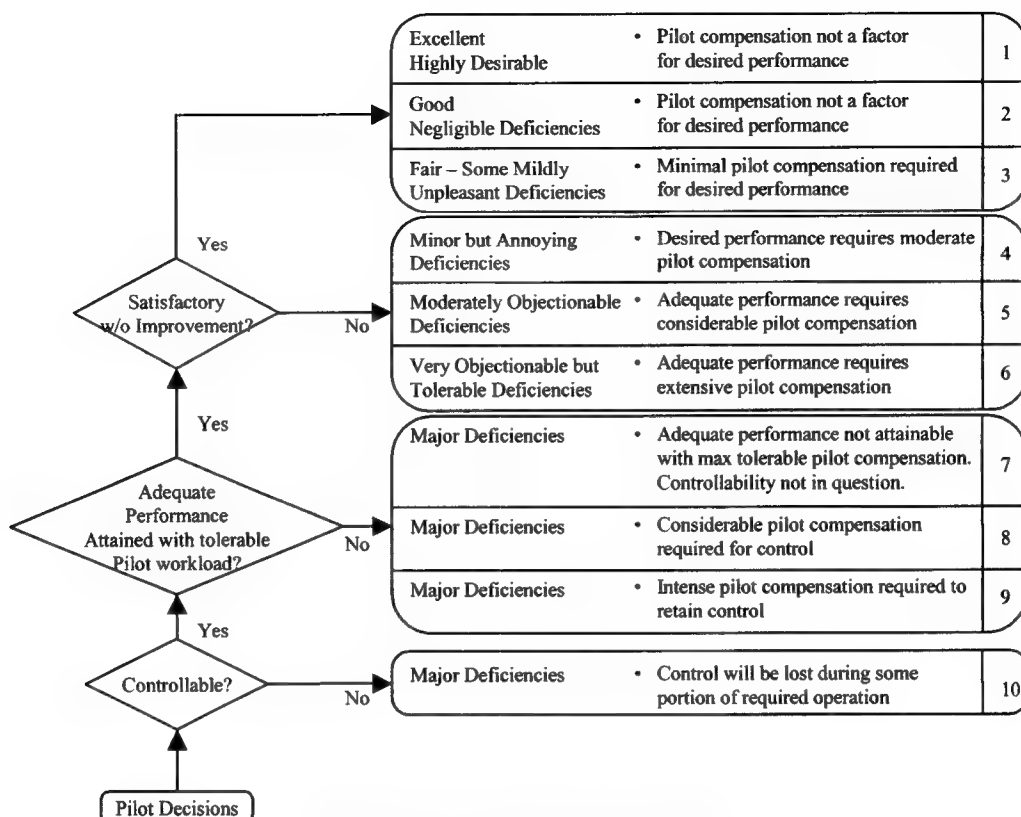


Figure I-6: Geometric Energy Height Loss for 105 KIAS Maneuvers

Note: Pilot 2 did not fly anti-hairpin maneuvers in a shear at 105 KIAS.

Appendix J: Cooper-Harper Rating Scale



Cooper-Harper Ref. NASA TND-5153

This page intentionally left blank.

Appendix K: Acronym List

| <u>Abbreviation</u> | <u>Definition</u> |
|---------------------|---------------------------------------|
| AFB | Air Force Base |
| AFIT | Air Force Institute of Technology |
| AGL | above ground level |
| AOA | angle of attack |
| AOS | angle of sideslip |
| D | drag |
| DAS | data acquisition system |
| DOE | design of experiments |
| DFRC | Dryden Flight Research Center |
| DS FTT | Dynamic Soaring flight test technique |
| E_s | specific energy height |
| FCIF | flight crew information file |
| ft | feet |
| FTE/N | flight test engineer |
| FTN | flight test navigator |
| g | acceleration due to gravity |
| GPS | global positioning system |
| GUI | graphical user interface |
| HOS | hands on stick |
| IMU | inertial measurement unit |
| INS | inertial navigation system |

| <u>Abbreviation</u> | <u>Definition</u> |
|---------------------|--|
| JON | job order number |
| KIAS | knots indicated air speed |
| L | lift |
| MSL | mean sea level |
| NASA | National Aeronautics and Space Administration |
| NOTAM | notice to airmen |
| PC | personal computer |
| POV | privately owned vehicle |
| RTD | resistive temperature detector |
| ShWOOPIN | Shear Wind Observed Optimized Investigation for NASA |
| SODAR | Sonic Detection and Ranging |
| TACAN | tactical air navigation |
| TIM | technical information memorandum |
| TMP | test management project |
| TPS | Test Pilot School |
| USAF | United States Air Force |
| VHF | very high frequency |

Distribution List

| OFFICE | Paper/PDF | NUMBER OF COPIES |
|--|--------------|------------------|
| AFFTC/HO 305 E Popson Ave, Bldg 1405 Edwards AFB, CA 93524-6595 | PDF | 1 |
| 412 TW/ENTL (AFFTC Technical Library) 307 E Popson Blvd, Bldg 1400, Room 110 Edwards AFB, CA 93524-6630 | Paper PDF | 1 1 |
| USAF TPS/EDT Attn: Mr. Gary Aldrich 220 S. Wolfe Blvd Edwards AFB, CA 93524-6485 | Paper PDF | 1 1 |
| USAF TPS/EDC Attn: Ms. Dottie Meyer 220 S. Wolfe Blvd Edwards AFB, CA 93524-6485 | Paper PDF | 1 1 |
| Defense Technical Information Center DTIC/OMI 8725 John J. Kingman Road, Suite 0944 Ft. Belvoir VA 22060-6218 | PDF | 1 |
| AFIT/ENY Attn: Maj Paul Blue 2950 Hobson Way Wright-Patterson AFB, OH 45433-7765 | Paper PDF | 1 1 |
| HQ AFMC/HO 4375 Chidlaw Road, Suite S231 Wright-Patterson AFB, OH 45433-5006 | PDF | 1 |
| 412 TW/ENFB Attn: Reagan Woolf 30 N Wolfe Ave, Bldg 1609 Edwards AFB, CA 93524-6843 | Paper PDF | 1 1 |

| OFFICE | Paper/PDF | NUMBER OF COPIES |
|---|----------------------------|------------------------|
| USAF TPS/EDT Attn: Lt Col Mark Stuckey 220 S. Wolfe Blvd. Edwards AFB, CA 93524-6485 | Paper PDF | 1 1 |
| Capt Randy Gordon 6836 Payne Ave Edwards AFB, CA 93523 | Paper PDF | 1 1 |
| Maj Jeff Fails Class 05B 220 S. Wolfe Blvd Edwards AFB, CA 93524-6485 | Paper PDF | 1 1 |
| Capt Solomon Baase 6825 Spaatz Dr. Edwards AFB, CA 93523 | Paper PDF | 1 1 |
| Capt Jason Eckberg USAF TPS/DOS 220 S. Wolfe Blvd Edwards AFB, CA 93524-6485 | Paper PDF | 1 1 |
| Capt Matt Ryan 6767 Rickenbacker Dr. Edwards, CA 93523 | Paper PDF | 1 1 |
| Capt Chris Smith 432 10 th St Edwards AFB, CA 93523 | Paper PDF | 1 1 |
| Capt Elwood Waddell 425 13 th Street Edwards, CA 93523 | Paper PDF | 1 1 |
| Total Copies | PDF Paper | 18 11 |